Compound Event-Triggered Distributed MPC for Coupled Nonlinear Systems

Yu Kang, *Senior Member, IEEE*, Tao Wang, Pengfei Li, Zhenyi Xu, and Yun-Bo Zhao, *Senior Member, IEEE*

***Abstract*—This article investigates the event-triggered distributed model predictive control (DMPC) for perturbed coupled nonlinear systems subject to state and control input constraints. A novel compound event-triggered DMPC strategy, including a compound triggering condition and a new constraint tightening approach, is developed. In this event-triggered strategy, two stability-related conditions are checked in a parallel manner, which relaxes the requirement of the decrease of the Lyapunov function. An open-loop prediction scheme to avoid periodic transmission is designed for the states in the terminal set. As a result, the number of triggering and transmission instants can be reduced significantly. Furthermore, the proposed constraint tightening approach solves the problem of the state constraint satisfaction, which is quite challenging due to the external disturbances and the mutual influences caused by dynamical coupling. Simulations are conducted at last to validate the effectiveness of the proposed algorithm.**

***Index Terms*—Coupled nonlinear systems, distributed model predictive control (DMPC), parallel triggered.**

I. Introduction

LARGE-SCALE systems that are mostly dynamically coupled have been actively studied due to their applications in many practical systems, for example, autonomous guided vessels, intelligent traffic systems, and water distribution systems [1], [2]. For such systems, conventional central model predictive control, a powerful control technique in handling system constraints and optimizing control performance, may fail to work due to the heavy computational load [1], calling for a more efficient control strategy. Distributed model predictive control (DMPC) is a promising strategy and the main idea of which is to decompose the original overall optimization problem into multiple individual optimal problems for the corresponding subsystems and then generate the control signal by exploiting the local information of each subsystem. As a consequence, the computational load can be significantly released. Therefore, DMPC has received much attention and found wide applications in recent years.

In DMPC for large-scale dynamically coupled systems, each subsystem directly impacts the others through the dynamic coupling, resulting in mutual disturbances. Such disturbances bring challenges to the design of the DMPC algorithm. In order to deal with the mutual influences, multitudinous researches have been carried out (see, for example, [3]–[12]). The design method of these work can be mainly categorized into two classes. The first is to treat the coupled states as external disturbances [3]–[7], and neglect them in the prediction model, for example, stabilizing the decentralized MPC algorithm in [3], tube-based MPC in [4], robust DMPC strategy with a new robust constraint in [5], communication-based DMPC approach in [6], and the novel cooperative DMPC method that improves the global cost function of each local controller in [7]. It is worth noting that there is no information exchange between the subsystems as the predicted states of each subsystem are always generated based on the nominal state dynamics of the subsystem, leading to a simpler algorithm design. However, information exchange helps to predict the dynamic behaviors of each subsystem more accurately, which is often beneficial to the control performance [13].

While in the second class, the information exchange is considered in predicting the future dynamic behaviors. To be specific, for a subsystem, its control input sequence is generated by solving its optimization problem based on its own information and that of its neighbors (a subset of other subsystems). In this way, the second design method is capable of achieving better control performance and receives great attention (see, e.g., [8]–[12]). To guarantee the state and control input constraints satisfaction, a tube-based DMPC approach for the linear disturbance-free system is proposed in [8], and a robust noniterative DMPC strategy for the perturbed linear system is developed in [9]. An iterative learning model predictive control framework for dynamically coupled linear multiagent systems is presented in [11]. To consider economic performance in the context of the standard MPC, a distributed

Manuscript received 20 December 2021; accepted 10 March 2022. Date of publication 25 March 2022; date of current version 18 August 2023. This work was supported in part by the National Key Research and Development Program of China under Grant 2018AAA0100801; in part by the National Natural Science Foundation of China under Grant 62033012, Grant 62103394, Grant 62173317, Grant 62103124, and Grant 61725304; in part by the Project funded by China Postdoctoral Science Foundation under Grant 2020M682036; and in part by the Science and Technology Major Project of Anhui Province under Grant 201903a07020012. This article was recommended by Associate Editor A. Katriniok. *(Corresponding authors: Tao Wang; Pengfei Li.)*

Yu Kang is with the Department of Automation, University of Science and Technology of China, Hefei 230027, China, and also with the Institute of Advanced Technology, University of Science and Technology of China, Hefei 230088, China (e-mail: kangduyu@ustc.edu.cn).

Tao Wang, Pengfei Li, and Yun-Bo Zhao are with the Department of Automation, University of Science and Technology of China, Hefei 230027, China (e-mail: wanghtao@mail.ustc.edu.cn; puffylee@ustc.edu.cn; ybzhao@ieee.org).

Zhenyi Xu is with the Institute of Artificial Intelligence, Hefei Comprehensive National Science Center, Hefei 230088, China (e-mail: xuzhenyi@ustc.edu.cn).

Color versions of one or more figures in this article are available at https://doi.org/10.1109/TCYB.2022.3159343.

Digital Object Identifier 10.1109/TCYB.2022.3159343

economic MPC algorithm is proposed in [12]. For coupled nonlinear systems, two new constraints on the current predicted state and the previous predicted state are introduced in the distributed optimization problem in [10] to guarantee the DMPC algorithm feasibility and the closed-loop stability. However, state constraints have not been considered in [10]. In fact, when considering the distributed implementation of coupled systems, the mutual influences will inevitably be encountered, which is a challenge for DMPC algorithm design.

Note that the aforementioned DMPC algorithms are based on the time-triggered mechanism, which may be impractical in actual environments with limited computation and communication resources, especially for large-scale systems. Therefore, a more computation- and communication-efficient control strategy is required for DMPC.

To deal with the above problem, event-triggered control is introduced. Event-triggered control has potential advantages in reducing communication resources because the control actuation is triggered only when certain prescribed conditions are violated rather than periodically. In this context, several types of event-triggered control strategies have been proposed, such as static event-triggered control [14], dynamic event-triggered control [15], mixed event-triggered control [16], and adaptive event-triggered control [17].

Motivated by the merit of event-triggered control, it is of great interest to apply event-triggered control to DMPC to form event-triggered DMPC as it can save communication and computation resources by reducing the amount of solving the distributed optimization problem and exchanging the local information. Recently, many event-triggered DMPC approaches have been developed, which can be classified according to system type (dynamically decoupled systems and dynamically coupled systems). Specifically, for dynamically decoupled systems, distributed periodic event-triggered strategy [18], adaptive event-triggered strategy [19], and dynamic event-triggered mechanism [20] have been proposed. Nevertheless, to the best of our knowledge, for coupled systems, very few results are reported with the exception of [21] and [22], though most of the practical large-scale systems are often comprised of dynamically coupled subsystems. This is because the coupling influences increases the difficulty of designing triggering strategy and analyzing system performance.

Although event-triggered DMPC for coupled systems has been studied in [21] and [22], there are some problems to be solved.

1) The triggering conditions designed to ensure the decrease of the Lyapunov function as time elapses (see, e.g., [20]–[22]) are easily met due to the use of many conservative inequalities especially in the presence of external disturbances. As a result, the computation resources cannot be saved effectively.
2) The dual-model strategy adopted in [18]–[22] requires the state information and control inputs to be transmitted periodically after the states enter the terminal set, resulting in a high communication load in many large-scale networked control systems [23]–[25].
3) The control parameters designed for different subsystems, such as the prediction horizon and the triggering threshold, are the same in the previous works [21], [22], [26]. In this way, the designed triggering conditions are relatively conservative due to the neglect of different characteristics between the subsystems.
4) Due to dynamic coupling, the conventional constraint tightening approach [27], [28] to guarantee the satisfaction of state constraint cannot work. As a result, state constraints, which exist in multiple practical large-scale processes, are not considered in most researches on coupled systems [8], [10], [21], [22].

Motivated by the above discussions, this article investigates event-triggered DMPC for perturbed coupled nonlinear systems subject to state and input constraints, aiming at designing an efficient event-triggered DMPC scheme to reduce the computation and communication load and ensure the satisfaction of constraints. The main contributions of our work are as follows.

1) A compound event-triggered DMPC strategy is designed for coupled nonlinear systems, which is computation and communication efficient, and does not need to keep the Lyapunov function decreasing compared with the one [21], [22].
2) A new constraint tightening approach is developed for the optimization problem. Compared with the results in [10], [21], and [22] where the state constraints are not considered, the approach in this work is capable of guaranteeing the satisfaction of the state constraints even in the presence of external disturbances.
3) Sufficient conditions for guaranteeing algorithm feasibility and closed-loop stability are derived, which enables the separate design of the control parameters for each subsystem, leading to lower conservative results.

The structure of this article is organized as follows. Section II describes the research problem. Section III gives the design of the compound event-triggered DMPC algorithm, including the distributed optimization problem and the compound triggering condition. The analysis of the algorithm feasibility and the closed-loop stability is shown in Section IV. Section V gives an illustrative example. Finally, Section VI concludes this article.

Notations: Let $\mathbb{R}$ and $\mathbb{N}$ denote the real and nonnegative integers, respectively, and $\mathbb{R}^n$ is the n-dimensional Euclidean space. For a given matrix P, $P > 0$ means that P is positive definite; $\underline{\lambda}(P)$ and $\bar{\lambda}(P)$ denote the minimum and maximum eigenvalues of the matrix P, respectively; $\|P\|$ denotes the induced 2-norm of P. For a vector x, its Euclidean norm is denoted by $\|x\| \coloneqq \sqrt{x^T x}$ and $\|x\|_P \coloneqq \sqrt{x^T P x}$ represents the P-weighted norm. For two sets $A, B \subseteq \mathbb{R}^n$, $A \oplus B \coloneqq \{a+b : a \in A, b \in B\}$ denotes the the Minkowski addition set, and $A \ominus B \coloneqq \{a : a + b \in A \ \forall b \in B\}$ denotes the Pontryagin difference set.

II. Problem Formulation

Consider a networked control system with the structure being depicted in Fig. 1, which is common and often used in practice (see, for example, [23]–[25]). The structure includes the plant that consists of multiple coupled subsystems, a cloud

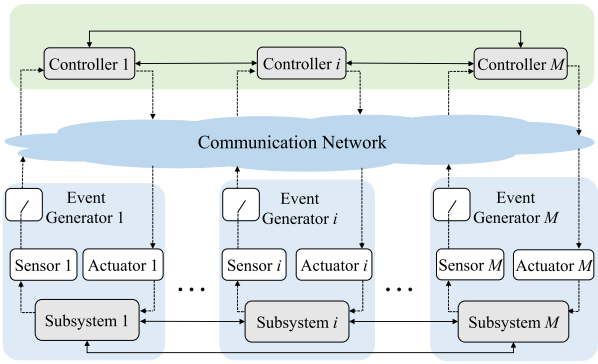

Fig. 1. Structure of event-triggered DMPC for networked control systems.

computing platform that consists of multiple decomposed controllers, and the networks between the local components (e.g., sensors, event generators, and actuators) and the remote controller. The entire executing procedure of the networked control system is elaborated as follows.

1) Each sensor i measures the state periodically, and the event generator i determines whether to transmit the measured state to the remote controller i via the communication network.
2) Each remote controller i solves an optimization problem only when the current state of subsystem i is received. The resultant optimal control inputs and the corresponding states are transmitted to the actuator i via the communication network.

Note that the information among the sensor i, the event generator i, and the actuator i is assumed to be shared. Similarly, the information between various controllers in the cloud computing platform is also assumed to be shared, which enables the controller i to use the information of i's neighbors in formulating the optimization problem. In practical systems, such information share can be realized in hardware without requiring communication costs.

In the following part, the system model is described in detail, and the problem to be investigated is elaborated.

The considered plant consists of M nonlinear discrete-time subsystems, which are coupled through states. The dynamic coupling between the subsystems is described by a directed graph $\mathcal{G} = (\mathcal{M}, \mathcal{E})$, where $\mathcal{M} = \{1, \ldots, M\}$ is the set of nodes and $\mathcal{E} \subset \mathcal{M} \times \mathcal{M}$ is the set of edges. The ith perturbed discrete-time subsystem subject to state and input constraints is given by

$$x_i(k+1) = f_i(x_i(k), u_i(k)) + \sum_{j \in \mathcal{N}_i^u} g_{ij}(x_j(k)) + w_i(k) \quad (1)$$

where $i \in \mathcal{M}$, $x_i(k) \in \mathcal{X}_i \subset \mathbb{R}^{n_i}$ and $u_i(k) \in \mathcal{U}_i \subset \mathbb{R}^{m_i}$ denote the state and control input of subsystem i, respectively, and $w_i(k) \in \mathcal{W}_i = \{w_i \in \mathbb{R}^{n_i} : \|w_i\|_{P_i} \leq \rho_i, \rho_i > 0\}$ is the external disturbance. The sets $\mathcal{X}_i$ and $\mathcal{U}_i$ are compact and contain the origin. The symbol $\mathcal{N}_i^u$ denotes the upstream neighbor of subsystem i, that is, the components of j's state appear in the dynamics of subsystem i for all subsystem $j, j \neq i$. On the contrary, subsystem i is an downstream neighbor of j, that is, $i \in \mathcal{N}_j^d$.

Moreover, the subsystem dynamics in (1) with $f_i(0, 0) = 0$ and $g_{ij}(0) = 0$ satisfy the following assumption.

Assumption 1: f_i and g_{ij} are local Lipschitz continuous with two constants L_{f_i} and $L_{g_{ij}}$, respectively. That is $\forall(\varsigma, \varphi, \zeta, \nu) \in \mathcal{X}_i \times \mathcal{X}_i \times \mathcal{X}_j \times \mathcal{X}_j$, $i \in \mathcal{M}$, and $j \in \mathcal{N}_i^u$ we have

$$\|f_i(\varsigma, u) - f_i(\varphi, u)\|_{P_i} \leq L_{f_i}\|\varsigma - \varphi\|_{P_i} \quad (2)$$

$$\|g_{ij}(\zeta) - g_{ij}(\nu)\|_{P_i} \leq L_{g_{ij}}\|\zeta - \nu\|_{P_i} \quad (3)$$

where P_i is the weighted matrix.

Remark 1: Unlike the work in [22], where the global Lipschitz constants are exploited, this article is allowed to use the local Lipschitz constants due to the state constraints. As a result, conservatism is reduced. Moreover, note that the local Lipschitz constant L_{f_i} is dependent on matrix-weighted P_i, we can use the same technique (change another matrix weighted) as in [29] to further reduce conservatism.

Based on the subsystem dynamics (1), the overall constrained coupled system can be expressed as the catenated vector form

$$\begin{aligned} x(k+1) &= F(x(k), u(k)) + w(k) \\ &= f(x(k), u(k)) + g(x(k)) + w(k) \end{aligned} \quad (4)$$

where $x = [x_1^T, \ldots, x_M^T]^T \in \mathcal{X} \subseteq \mathbb{R}^n$, $\mathcal{X} = \mathcal{X}_1 \times \cdots \times \mathcal{X}_M$, $n = \sum_{i \in \mathcal{M}} n_i$, and $u = [u_1^T, \ldots, u_M^T]^T \in \mathcal{U} \subseteq \mathbb{R}^m$, $\mathcal{U} = \mathcal{U}_1 \times \cdots \times \mathcal{U}_M$, $m = \sum_{i \in \mathcal{M}} m_i$, and $w = [w_1^T, \ldots, w_M^T]^T \in \mathcal{W} \subseteq \mathbb{R}^n$, $\mathcal{W} = \mathcal{W}_1 \times \cdots \times \mathcal{W}_M$. Furthermore, $f(x, u) = [f_1(x_1, u_1)^T, \ldots, f_M(x_M, u_M)^T]^T$ and $g(x) = [\sum_{j \in \mathcal{N}_1^u} g_{1j}(x_j)^T, \ldots, \sum_{j \in \mathcal{N}_M^u} g_{Mj}(x_j)^T]^T$.

To stabilize the closed-loop system inside a neighborhood of the origin, a linear local controller whose design depends on the linearization of (1) is adopted. Furthermore, the terminal set, where the local controller will be used, can be defined based on the linearization of (4). To that end, the linearization of (1) and (4) is introduced.

The linearized dynamics of subsystems i around the origin is denoted as

$$x_i(k+1) = A_{ii}x_i(k) + B_i u_i(k) + \sum_{j \in \mathcal{N}_i^u} A_{ij}x_j(k) + w_i(k) \quad (5)$$

where $A_{ii} = \partial f_i/\partial x_i(0, 0)$, $A_{ij} = \partial g_{ij}/\partial x_j(0)$ for $j \in \mathcal{N}_i^u$, and $B_i = \partial f_i/\partial u_i(0, 0)$. The linearized dynamics of (4) are formulated as

$$x(k+1) = Ax(k) + Bu(k) + w(k) \quad (6)$$

where $A = \partial F/\partial x(0, 0)$, $B = \partial f/\partial u(0, 0)$.

Assumption 2: For each linearized subsystem in (5), there exists a feedback controller $u_i(k) = K_i x_i(k)$ such that $A_{s_i} = A_{ii} + B_i K_i$ and $A_o = A + BK$ are both Schur, where $K = \text{diag}(K_1, \ldots, K_M)$.

The remainder of this section states the main research objective of this work.

From the executing procedure of the networked control system shown in Fig. 1, the consumption of the communication and computation resources is related to the frequencies of transmitting data and solving the optimization problem. Therefore, the main objective is to design an event-triggered

DMPC strategy to reduce the number of triggering instants, thereby reducing communication and computation load.

Remark 2: Note that the controller of each subsystem is placed at local side in [21] and [22], but at remote side in Fig. 1. Such difference leads to two influences as follows.

1) The information exchange between different subsystems in [21] and [22] requires the communication network. However, such a requirement is not needed in Fig. 1 since the information exchange between remote controllers is realized in hardware.
2) For each subsystem i, the information transmission from the controller i to its local components does not require the use of communication resources in [21] and [22], but the control structure in Fig. 1 does.

III. Compound Event-Triggered DMPC

In this section, the optimization problem of each subsystem is formulated first, and then derive the compound triggering conditions based on feasibility and stability. The overall event-triggered DMPC algorithm is presented at the end.

A. Optimization Problem

Under the event-triggered DMPC framework, all controllers are activated asynchronously, since the triggering instants of each subsystem are distinct. As a result, for each controller i, the actual state information of its upstream neighbors $j(j \in \mathcal{N}_i^u)$, which is beneficial to control performance, is not available.

For each subsystem i, let $k_i^r, r \in \mathbb{N}$ denote its rth triggering instant. To reject the mutual influences, each subsystem i should presume its upstream neighbors' behaviors. Specifically, to that end, prior to each triggering instant k_i^r, each controller i uses its upstream neighbors' assumed states, denoted by $\tilde{x}_j$. Similarly, subsystem i shares its assumed state $\tilde{x}_i$ to its downstream neighbors.

The local optimization problem $\mathcal{P}_i$ is defined by

$$\mathcal{P}_i: \min_{\hat{\mathbf{u}}_i(k_i^r)} \; J_i\big(\hat{x}_i(k_i^r), \hat{\mathbf{u}}_i(k_i^r), N_i\big)$$

$$\text{s.t. } \hat{x}_i\big(k_i^r+m+1|k_i^r\big) = f_i\big(\hat{x}_i\big(k_i^r+m|k_i^r\big), \hat{u}_i\big(k_i^r+m|k_i^r\big)\big) + \sum_{j\in\mathcal{N}_i^u} g_{ij}\big(\tilde{x}_j(k_i^r+m|k_i^r)\big), m=0,\ldots,N_i-1 \tag{7a}$$

$$\Big\|\hat{x}_i\big(k_i^r+m|k_i^r\big) - \bar{x}_i^*\Big(k_i^r+m|k_i^{r-1}\Big)\Big\|_{P_i} \le \sigma \quad m=0,\ldots,N_i \tag{7b}$$

$$\hat{x}_i\big(k_i^r+m|k_i^r\big) \in \mathcal{X}_i \ominus \mathcal{B}_i(m), m=1,\ldots,N_i-1 \tag{7c}$$

$$\hat{u}_i\big(k_i^r+m|k_i^r\big) \in \mathcal{U}_i, m=0,\ldots,N_i-1 \tag{7d}$$

$$\hat{x}_i\big(k_i^r+N_i|k_i^r\big) \in \phi_i\Big(\tfrac{4\varepsilon}{5}\Big) \tag{7e}$$

where N_i is the prediction horizon of subsystem i. $\hat{\mathbf{u}}_i(k_i^r) = \{\hat{u}_i(k_i^r|k_i^r), \ldots, \hat{u}_i(k_i^r+N-1|k_i^r)\}$ is the predicted control input sequence at time k_i^r, and $\phi_i(4\varepsilon/5) = \{x \in \mathbb{R}^{n_i} : \|x\|_{P_i} \le 4\varepsilon/(5\sqrt{M})\}$ denotes the terminal set. The positive control parameters ε and σ are to be determined.

Denote $\hat{\mathbf{u}}_i^*(k_i^r) = \{\hat{u}_i^*(k_i^r|k_i^r), \ldots, \hat{u}_i^*(k_i^r+N_i-1|k_i^r)\}$ by the optimal control input sequence, and $\hat{\mathbf{x}^*}_i(k_i^r) = \{\hat{x}_i^*(k_i^r|k_i^r), \ldots, \hat{x}_i^*(k_i^r+N|k_i^r)\}$ the corresponding optimal predicted state sequence. Define $\Delta(k_i^r) = k_i^r - k_i^{r-1}$. The following part specifies the expression of $\tilde{x}_j(k_i^r+m|k_i^r)$, $\bar{x}_i^*(k_i^r+m|k_i^{r-1})$, $\mathcal{B}_i(m)$, and $J_i(\hat{x}_i(k_i^r), \hat{\mathbf{u}}_i(k_i^r), N_i)$ in $\mathcal{P}_i$, respectively.

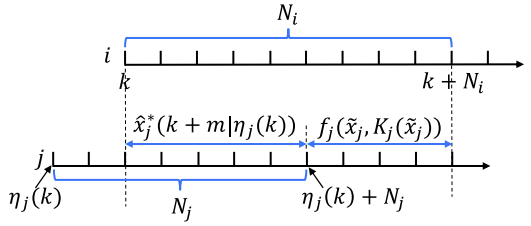

Fig. 2. Illustration of constructing the assumed state.

1) The assumed state $\tilde{x}_j(k+m|k), j \in \mathcal{N}_i^u$ is constructed by

$$\tilde{x}_j(k+m|k) = \begin{cases} \hat{x}_j^*(k+m|\eta_j(k)), m=0,\ldots,\eta_j(k)+N_j-k \\ f_j\big(\tilde{x}_j(k+m-1|k), K_j\tilde{x}_j(k+m-1|k)\big) \\ \qquad m=\eta_j(k)+N_j-k+1,\ldots,N_i \end{cases} \tag{8}$$

where $\eta_j(k)$ is the latest triggering instant of subsystem j before k, that is, $\eta_j(k) < k$. Fig. 2 gives an illustration of constructing the assumed state.

2) The state $\bar{x}_i^*(k_i^r+m|k_i^{r-1})$ in (7b) is constructed by

$$\bar{x}_i^*\Big(k_i^r+m|k_i^{r-1}\Big) = \begin{cases} \hat{x}_i^*\Big(k_i^r+m|k_i^{r-1}\Big), & k=0,\ldots,N_i-\Delta\big(k_i^r\big) \\ f_i\Big(\bar{x}_i^*\Big(k_i^r+m-1|k_i^{r-1}\Big), K_i\bar{x}_i^*\Big(k_i^r+m-1|k_i^{r-1}\Big)\Big) \\ \qquad k=N_i-\Delta\big(k_i^r\big)+1,\ldots,N_i. \end{cases}$$

3) The tightened set $\mathcal{B}_i(m)$ is defined as

$$\mathcal{B}_i(m) := \left\{x \in \mathbb{R}^{n_i} : \|x\|_{P_i} \le \tfrac{L_{f_i}^m-1}{L_{f_i}-1}\tau_i + N_i\Gamma_i L_{g_{ij}}\sigma\tfrac{L_{f_i}^m-L_{f_i}}{(L_{f_i}-1)^2}\right\} \tag{9}$$

where τ_i is a positive constant that will be determined latter.

4) The cost function in $\mathcal{P}_i$ is defined as

$$J_i\big(\hat{x}_i\big(k_i^r\big), \hat{\mathbf{u}}_i\big(k_i^r\big), N_i\big) = \sum_{m=0}^{N_i-1}\big\|\hat{x}_i\big(k_i^r+m|k_i^r\big)\big\|_{Q_i}^2 + \big\|\hat{u}_i\big(k_i^r+m|k_i^r\big)\big\|_{R_i}^2 + \big\|\hat{x}_i\big(k_i^r+N_i|k_i^r\big)\big\|_{P_i}^2 \tag{10}$$

where Q_i, R_i, and P_i are positive-definite matrices. Furthermore, P_i satisfies the Lyapunov equation $A_{s_i}^T P_i A_{s_i} - P_i = -(\tilde{Q}_i + \Delta Q_i)$, where $\tilde{Q}_i = Q_i + K_i^T R_i K_i$, and ΔQ_i is a positive-definite matrix.

Remark 3:

1) The constraint in (7b) implies that the predicted state $\hat{x}_i(k_i^r+m|k_i^r)$ of subsystem i does not diverge far away from $\bar{x}^*(k_i^r+m|k_i^{r-1})$. By imposing this constraint, the relationship between the feasible state to be constructed and the optimal predicted state can be established, thus facilitating the feasibility analysis of the optimization problem $\mathcal{P}_i$.
2) The tightened set $\mathcal{B}_i(m)$ in (9) is defined to ensure $x_i(k) \in \mathcal{X}_i \; \forall k > 0$ in the presence of mutual and external disturbances, which will be shown in Section IV.

The assumptions of the degree of coupling and the state feedback gain are as follows.

Assumption 3: $A_o^T P A_o - A_s^T P A_s \leq 1/2\tilde{Q}$.

Assumption 4: There exist an auxiliary set $\phi_i(\varepsilon)$ with the form of $\phi_i(\varepsilon) := \{x_i : \|x_i\|_{P_i} \leq \varepsilon/\sqrt{M}\}$ and several constants $L_{f_{K_i}} > 0$, $0 < c_i < 1$, and $0 < \alpha_i < 1$, such that for all $i \in \mathcal{M}, j \in N_i^u$:

1) $\phi_i(\varepsilon) \subseteq \{x_i \in \mathcal{X}_i \ominus \mathcal{B}_i(N_i - 1) : K_i x_i \in \mathcal{U}_i\}$;
2) $f_i(x_i, K_i x_i) \in \phi_i(4c_i\varepsilon/5)\ \forall x_i \in \phi_i(4\varepsilon/5)$;
3) $f_i(x_i, K_i x_i) + \sum_{j \in \mathcal{N}_i^u} g_{ij}(\tilde{x}_j) \in \phi_i(\alpha_i \varepsilon)\ \forall x_i \in \phi_i(\varepsilon)$, and $\tilde{x}_j \in \phi_j(\varepsilon)$;
4) $\|f_i(x_i, K_i x_i) - f_i(y_i, K_i y_i)\|_{P_i} \leq L_{f_{K_i}} \|x_i - y_i\|_{P_i}\ \forall x_i, y_i \in \phi_i(\varepsilon)$.

Remark 4:

1) Assumption 3 is a standard assumption adopted in much DMPC literature (see, e.g., [5], [10], and [22]). It limits the degree of coupling between subsystems and is a prerequisite for the existence of a positively invariant set $\phi(\varepsilon)$ in Lemma 1 and can be satisfied if the positive-definite matrix ΔQ is chosen appropriately.
2) The properties 1)–4) in Assumption 4 are proposed to guarantee the recursive feasibility of the optimization problem and the stability of the overall system. The properties 1), 2), and 4) are standard (see, e.g., [9], [26]–[28], [30]). Property 1) holds as long as $\phi_i(\varepsilon)$ is set to be small. Property 2) can be easily satisfied by setting $c_i = \sqrt{1 - \bar{\lambda}(P_i^{-1/2} \tilde{Q}_i P_i^{-1/2})}$ according to Lemma 1. Property 3) is similar to the assumptionsin [9] and [26] and may not be satisfied when the degree of coupling between subsystems is too strong [5], [10], [22]. In addition, determining α_i analytically for a coupled nonlinear system is an intractable task. Instead, we can find α_i via numerical simulations.

Lemma 1: Let $A_s = \text{diag}(A_{s_1}, \ldots, A_{s_M})$, $Q = \text{diag}(Q_1, \ldots, Q_M)$, $R = \text{diag}(R_1, \ldots, R_M)$, $P = \text{diag}(P_1, \ldots, P_M)$, and $\Delta Q = \text{diag}(\Delta Q_1, \ldots, \Delta Q_M)$. Then, for the system $x(k+1) = F(x(k), Kx(k))$ with Assumptions 1-3:

1) there exists a constant ε such that the set $\phi(\varepsilon) := \{x : V(x) \leq \varepsilon^2\}$ is a positively invariant set;
2) $V(x(k+1)) - V(x(k)) \leq -1/2 x(k)^T \tilde{Q} x(k)$ hold for any $x(k) \in \phi(\varepsilon), Kx(k) \in \mathcal{U}$, where $V(x(k)) = \|x(k)\|_P^2$.

Proof: This proof follows similar logic of [31], but we still sketch here since some steps will be helpful in the following design. Define $\psi(x(k)) = F(x(k), K(x(k))) - A_o(x(k))$, then difference of $V(x(k))$ along the trajectory $x(k+1) = F(x(k), K(x(k)))$ can be calculated as

$$\begin{aligned} &V(x(k+1)) - V(x(k)) \\ &= x(k)^T A_o^T P A_o x(k) + \psi(x(k))^T P \psi(x(k)) \\ &\quad + 2\psi(x(k))^T P A_o x(k) - x(k)^T P x(k). \end{aligned}$$

Considering $A_s^T P A_s - P = -(\tilde{Q} + \Delta Q)$ and $A_o^T P A_o - A_s^T P A_s \leq 1/2\tilde{Q}$, we have

$$\begin{aligned} &V(x(k+1)) - V(x(k)) \\ &\leq -\frac{1}{2} x(k)^T \tilde{Q} x(k) - x(k)^T \Delta Q x(k) \\ &\quad + \psi(x(k))^T P \psi(x(k)) + 2\psi(x(k))^T P A_o x(k). \end{aligned} \tag{11}$$

The terms involving $\psi(x(k))$ in the above inequality is bounded as follows:

$$\begin{aligned} \psi(x(k))^T P \psi(x(k)) &\leq \|P\| \cdot L_\phi^2 \cdot \|x(k)\|^2 \\ \psi(x(k))^T P A_o x(k) &\leq \|P A_o\| \cdot \|\psi(x(k))^T\| \cdot \|x(k)\| \\ &\leq \|P A_o\| \cdot L_\phi \cdot \|x(k)\|^2 \end{aligned} \tag{12}$$

where $L_\phi := \sup\{\|\psi(x)\|/\|x\| | x \in \phi(\varepsilon), x \neq 0\}$.

Substituting (12) into (11) yields

$$\begin{aligned} V(x(k+1)) - V(x(k)) \leq &-\frac{1}{2} x(k)^T \tilde{Q} x(k) - x(k)^T \Delta Q x(k) \\ &+ \left(L_\phi^2 \|P\| + 2L_\phi \|P A_o\|\right) \|x(k)\|^2. \end{aligned}$$

Thus, 1) and 2) both hold if the following condition holds:

$$\left(L_\phi^2 \|P\| + 2L_\phi \|P A_o\|\right) \|x(k)\|^2 \leq x(k)^T \Delta Q x(k).$$

Since $x(k)^T \Delta Q x(k) \geq \underline{\lambda}(\Delta Q) \|x(k)\|^2$, the above condition is equivalent to

$$\underline{\lambda}(\Delta Q) - L_\phi^2 \|P\| - 2L_\phi \|P A_o\| \geq 0.$$

The positive solution of $L_\phi^2 \|P\| + 2L_\phi \|P A_o\| - \underline{\lambda}(\Delta Q) = 0$ is given as

$$L_\phi^* = \frac{\sqrt{\|P A_o\|^2 + \underline{\lambda}(\Delta Q)\|P\|} - \|P A_o\|}{\|P\|}.$$

Therefore, if we choose $\varepsilon > 0$ such that $L_\phi \leq L_\phi^*$, then the assertions 1) and 2) hold. This proof is completed. ■

Remark 5: The level set $\phi(\varepsilon)$ is crucial in constructing a feasible solution to the optimization problem as the horizon window moves to every computation cycle and is also important in analyzing the closed-loop stability (see, e.g., [10], [30]). To determine the level set $\phi(\varepsilon)$, we can choose the largest possible value of ε such that $L_\phi \leq L_\phi^*$. In addition, we can use an alternative approach to obtain a less conservative set $\phi(\varepsilon)$. In fact, in order to guarantee $V(x(k+1)) - V(x(k)) \leq -1/2 x(k)^T \tilde{Q} x(k)$, the inequality $-x(k)^T \Delta Q x(k) + \psi(x(k))^T P \psi(x(k)) + 2\psi(x(k))^T P A_o x(k) \leq 0$ in (11) should be met. Therefore, the control parameter ε is chosen such the optimal value $M(\varepsilon)$ of the following optimization problem remains negative:

$$\begin{aligned} M(\varepsilon) = \max_x\ &\left\{-x^T \Delta Q x + \psi(x)^T P \psi(x) + 2\psi(x)^T P A_o x\right\} \\ \text{s.t.}\ &0 < x^T P x \leq \varepsilon^2 \\ &\varepsilon \leq \zeta \end{aligned} \tag{13}$$

where ζ is designed such that $Kx \in \mathcal{U}\ \forall x \in \{x : x^T P x \leq \zeta\}$. To obtain a larger level set, one can increase the value of ε while keeping $M(\varepsilon)$ negative.

B. Compound Event-Triggering Condition

In this part, the compound triggering condition is determined, including a condition to ensure the recursive feasibility and a parallel-triggering condition to guarantee stability.

1) Triggering Condition for Feasibility: At every update time, for each subsystem i, the assumed state information of its upstream neighbors can be transmitted to subsystem i by controller i. In this case, the subsystem i can obtain the assumed state information of its upstream neighbors but not the actual one. Furthermore, the dynamics of subsystem i is subject to external disturbances. These two aspects lead to an estimated error between i's the predicted state and actual one, making the state constraints in (7b) and (7e) unsatisfaction. To circumvent this, the following triggering condition is proposed:

$$\left\|x_i(k)-\hat{x}_i^*\left(k|k_i^r\right)\right\|_{P_i}>\frac{\tau_i-\bar{\lambda}\left(P_i^{\frac{1}{2}}\right)\rho_i-\Gamma_i L_{g_{ij}}\left(\tau_j+N_i\sigma\right)}{L_{f_i}} \tag{14}$$

where $\Gamma_i=\max_{i\in\mathcal{M}}\text{Card}\{\mathcal{N}_i^u\}$.

For each subsystem $i, i\in\mathcal{M}$, if the deviation between its predicted state $\hat{x}_i^*(k|k_i^r)$ and actual state $x_i(k)$ exceeds the designed threshold, the event is triggered. Based on such triggering condition, the upper bound of the estimated error at the next triggering instant is given.

Lemma 2: For the subsystem in (1) with Assumption 1, if the triggering condition is designed as (14), then

$$\left\|x\left(k_i^{r+1}\right)-\hat{x}_i^*\left(k_i^{r+1}|k_i^r\right)\right\|_{P_i}\le\tau_i. \tag{15}$$

Proof: See Appendix A. ∎

This lemma shows that even if the event is triggered, the state error at the triggering instant is still bounded by τ_i, and this lemma is a preparation for the recursive feasibility.

2) Parallel-Triggering Condition for Stability: The essential spirit of designing the triggering condition to ensure stability lies in making the Lyapunov function decrease as time elapses.

Suppose that $\mathcal{P}_i$ in (7) is solved at the triggering instant k_i^r, the optimal solution $\hat{\mathbf{u}}_i^*(k_i^r)$ and the corresponding optimal state sequence $\hat{\mathbf{x}}_i^*(k_i^r)$ are obtained. Based on the optimal solution, the future control input sequence $\bar{\mathbf{u}}_i(k)=\{\bar{u}_i(k|k),\ldots,\bar{u}_i(k+N_i-1|k)\}$ and the corresponding state sequence $\bar{\mathbf{x}}_i(k)=\{\bar{x}_i(k_i^r|k_i^r),\ldots,\bar{x}_i(k_i^r+N|k_i^r)\}$ can be constructed as follows.

For $k=k_i^r+1$

$$\begin{cases}\bar{x}_i(k+m+1|k)=f_i(\bar{x}_i(k+m|k),\bar{u}_i(k+m|k))\\ \quad+\sum_{j\in\mathcal{N}_i^u}g_{ij}\left(\tilde{x}_j(k+m|k)\right),\ m=0,\ldots,N_i-1\\ \bar{u}_i(k+m|k)=\begin{cases}\hat{u}_i^*\left(k+m|k_i^r\right), & m=0,\ldots,N_i-2\\ K_i\bar{x}_i(k+m|k), & m=N_i-1.\end{cases}\end{cases} \tag{16}$$

For $k>k_i^r+1$

$$\begin{cases}\bar{x}_i(k+m+1|k)=f_i(\bar{x}_i(k+m|k),\bar{u}_i(k+m|k))\\ \quad+\sum_{j\in\mathcal{N}_i^u}g_{ij}\left(\tilde{x}_j(k+m|k)\right),\ m=0,\ldots,N_i-1\\ \bar{u}_i(k+m|k)=\begin{cases}\bar{u}_i(k+m|k-1), & m=0,\ldots,N_i-2,\\ K_i\bar{x}_i(k+m|k), & m=N_i-1\end{cases}\end{cases} \tag{17}$$

with $\bar{x}_i(k|k)=x_i(k)$, and $K_i(\cdot)$ is defined in Assumption 2. The constructed control input sequence $\bar{\mathbf{u}}_i(k)$ and state sequence $\bar{\mathbf{x}}_i(k)$ are utilized not only to determine the next triggering instant but also to analyze the recursive feasibility.

The Lyapunov function candidate is defined as

$$V_i(x_i(k|k))=\sum_{m=0}^{N_i}\|x_i(k+m|k)\|_{P_i}. \tag{18}$$

Denote the difference of the Lyapunov function between two successive time k and $k-1$ by $\Delta V_i(k)$, then

$$\Delta V_i(k)=\begin{cases}V_i(\bar{x}_i(k|k))-V_i\left(\hat{x}_i^*\left(k_i^r|k_i^r\right)\right), & k=k_i^r+1\\ V_i(\bar{x}_i(k|k))-V_i(\bar{x}_i(k-1|k-1)), & k_i^r+1<k<k_i^{r+1}.\end{cases}$$

In the following lemma, the upper bound of $\Delta V_i(k)$ is derived, which facilitates the triggering condition design.

Lemma 3: For each subsystem in (1) with Assumptions 1 and 4, if the constructed control inputs $\bar{\mathbf{u}}_i(k)$ from (16) or (17) are applied, then the upper bound of $\Delta V_i(k)$ is

$$\begin{aligned}\Delta V_i(k)\le&-\|x_i(k-1)\|_{P_i}+e_i(k)\\&+\sum_{m=1}^{N_i-1}\chi_i(m)+\left\|\hat{x}_i(k+N_i|k-1)\right\|_{P_i}\\&+L_{f_{K_i}}\chi_i(N_i-1)+\sum_{j\in\mathcal{N}_i^u}L_{g_{ij}}\xi_j(k+N_i-1|k)\end{aligned}$$

where

$$e_i(k)=\begin{cases}\left\|x_i(k)-\hat{x}_i^*\left(k|k_i^r\right)\right\|_{P_i}, & k=k_i^r+1\\ \|x_i(k)-\bar{x}_i(k|k-1)\|_{P_i}, & k_i^r+1<k<k_i^{r+1}\end{cases}$$

$$\chi_i(m)=L_{f_i}^m e_i(k)+\sum_{j\in\mathcal{N}_i^u}\sum_{l=0}^{m-1}L_{f_i}^{m-l-1}L_{g_{ij}}\xi_j(k+l|k)$$

$$\xi_j(k+l|k)=\|\tilde{x}_j(k+l|k)-\tilde{x}_j(k+l|k-1)\|_{P_i}$$

and

$$\hat{x}_i(k+N_i|k-1)=\begin{cases}f_i\left(\hat{x}_i^*\left(k+N_i-1|k_i^r\right),K_i\hat{x}_i^*\left(k+N_i-1|k_i^r\right)\right)\\ \quad+\sum_{j\in\mathcal{N}_i^u}g_{ij}\left(\tilde{x}_j\left(k+N_i-1|k_i^r\right)\right), & k=k_i^r+1\\ f_i(\bar{x}_i(k+N_i-1|k-1),K_i\bar{x}_i(k+N_i-1|k-1))\\ +\sum_{j\in\mathcal{N}_i^u}g_{ij}\left(\tilde{x}_j(k+N_i-1|k-1)\right), & k_i^r+1<k<k_i^{r+1}.\end{cases}$$

Proof: See Appendix B. ∎

According to Lemma 3, the triggering condition at time k is designed as follows to keep the stability by subjecting $V_i(x_i(k|k))$ to decrease:

$$\begin{aligned}&\sum_{m=1}^{N_i-1}\chi_i(m)+\left\|\hat{x}_i(k+N_i|k-1)\right\|_{P_i}+L_{f_{K_i}}\chi_i(N_i-1)\\&\quad+\sum_{j\in\mathcal{N}_i^u}L_{g_{ij}}\xi_j(k+N_i-1|k)+e_i(k)>\beta_i\|x_i(k-1)\|_{P_i}\end{aligned} \tag{19}$$

where $\beta_i\in(0,1)$ is a constant.

With the triggering condition (19), the Lyapunov function candidate is monotonically decreasing during $[k_i^r,k_i^{r+1}-1]$. However, this condition is easily met, especially in the presence of the external and mutual disturbances because the value of $\beta_i\|x_i(k-1)\|_{Q_i}^2$ is very small as the state $x_i(k)$ approaches the origin (see, e.g., [32]). As a consequence, the event is triggered frequently if the algorithm is performed only relies on

Algorithm 1 Compound Event-Triggered DMPC Algorithm

Initialization: For each subsystem, give initial state $x_i(0)$; calculate weighted matrices Q_i, R_i, P_i, local feedback gain K_i, and the level set $\phi_i(\varepsilon)$ according to Lemma 1; choose the prediction horizon N_i and control parameters τ_i, δ_i based on (25), (24) and (33); let $\theta_i = 0$ (θ is the switching signal, and $\theta = 1$ means the system state enters the level set).

1: For each controller i, at any time k, generate $\tilde{x}_j(k+m|k), m = 0, \ldots, N_i$ based on (8).
2: Measure the system state $x_i(k)$; check whether the triggering conditions in (22) hold true, if they hold, set $k_i^{r+1} = k$, $r = r+1$, receive $\hat{\mathbf{x}}_j^*(\eta_j(k))$ or $\hat{\mathbf{x}}_i(\eta_j(k))$ and update $\tilde{x}_j(k+m|k)$, go to step 3. Otherwise, go to 5.
3: If $\theta_i = 0$, solve $\mathcal{P}_i$ to obtain the optimal control and state sequence $\hat{\mathbf{u}}_i^*(k)$ and $\hat{\mathbf{x}}_i^*(k)$; apply $u_i(k) = \hat{u}_i^*(k|k)$ to the subsystem i, go to step 1. Otherwise, go to step 4.
4: Generate control sequence $\hat{u}_i(k+m|k), m = 0, \ldots, N_i-1$ and state sequence $\hat{\mathbf{x}}_i(k)$ according to (23); apply $u_i(k) = \hat{u}_i(k|k)$ to the subsystem i; set $\theta_i = 1$, go to step 1.
5: If $x_i(k) \in \phi_i(\varepsilon)$ and $\theta_i = 0$, go to step 4. Otherwise, go to step 6.
6: Construct $\bar{u}_i(k+m|k), m = 0, \ldots, N_i - 1$ based on (16) or (17); apply $u_i(k) = \bar{u}_i(k|k)$ to the subsystem; set $k = k+1$, go to step 1.

(20), resulting in high computation and communication load. Inspired by [33], we further propose the following auxiliary condition to reduce the triggering frequency:

$$\|x_i(k)\|_{P_i} > e^{-\gamma_i k}\|x_i(0)\|_{P_i} + \delta_i \tag{20}$$

where $x_i(0)$ is the initial state of subsystem i, $\gamma_i > 0$ and $0 < \delta_i < \varepsilon/\sqrt{M}$ are two constants

Then, combining (19) and (20) forms the following parallel-triggering condition:

$$\begin{cases} (19) & \text{(21a)} \\ \|x_i(k)\|_{P_i} > e^{-\gamma_i k}\|x_i(0)\|_{P_i} + \delta_i. & \text{(21b)} \end{cases}$$

In the majority of the event-triggered MPC literature, such as [21] and [34], an event occurs as long as the condition similar to (19) holds. But in our proposed triggering condition (21), only when both (19) and (20) are satisfied will an event be triggered. In this way, the proposed parallel-triggering condition (21) reduces the number of triggering instants further while achieving comparable control performance.

Summarizing the above triggering conditions (14) and (21), the compound triggering conditions are designed as

$$(14) \text{ or } (21) \text{ or } k - k_i^r \geq N_i. \tag{22}$$

If one of the conditions in (22) holds, the optimization problem $\mathcal{P}_i$ of subsystem i is solved and the triggering instant is updated to $k_i^{r+1} = k$. The more specific procedure is summarized in Algorithm 1.

C. Compound Event-Triggered DMPC Algorithm

To stabilize the overall systems, the state feedback gain K_i is adopted. However, in the control structure shown in Fig. 1, the implementation of the traditional dual-model strategy [18], [27] requires the periodic transmission of the system state and control input, resulting in a significant consumption of the communication resources. To overcome this issue, we employ the state feedback gain K to generate the predicted control inputs sequence in an open-loop manner when the system state enters the level set $\phi(\varepsilon)$, as follows:

$$\begin{cases} \hat{u}_i(k_i^r + m|k_i^r) = K_i(\hat{x}_i(k_i^r + m|k_i^r)) \\ \hat{x}_i(k_i^r + m + 1|k_i^r) = f_i(\hat{x}_i(k_i^r + m|k_i^r), \hat{u}_i(k_i^r + m|k_i^r)) \\ \qquad + \sum_{j\in\mathcal{N}_i^u} g_{ij}(\tilde{x}_j(k_i^r + m|k_i^r)) \end{cases} \tag{23}$$

where $m = 0, \ldots, N_i - 1$, $\hat{x}_i(k_i^r|k_i^r) = x_i(k_i^r)$, and k_i^r is the time when the state enters the level set.

The compound event-triggered DMPC algorithm is presented in Algorithm 1. For each subsystem i, at each triggering instant k_i^r, its upstream neighbors' state information is updated according to (8). If $x_i \notin \phi_i(\varepsilon)$, the control input sequence $\hat{\mathbf{u}}_i^*(k_i^r)$ is generated by solving $\mathcal{P}_i$ in (7). Otherwise, the control input sequence $\hat{\mathbf{u}}_i(k_i^r)$ is obtained according to (23). Then, the control input in $\hat{\mathbf{u}}_i^*(k_i^r)$ or $\hat{\mathbf{u}}_i(k_i^r)$ is applied to the subsystem i in turn until one of the conditions in (22) is satisfied, and the corresponding state trajectory $\hat{\mathbf{x}}_i^*(k_i^r)$ or $\hat{\mathbf{x}}_i(k_i^r)$ is transmitted to i's downstream neighbours. It is worth noting that, for $x_i(k_i^r) \notin \phi_i(\varepsilon)$, once the state $x_i(k), k > k_i^r$ enters the level set $\phi_i(\varepsilon)$, the event is triggered and the triggering instant is updated to $k_i^{r+1} = k$ even if the triggering condition (22) is not satisfied.

IV. Analysis

In this section, the satisfaction of the actual state constraints is validated, followed by recursive feasibility and stability analysis.

A. Actual State Constraints Analysis

In general, due to the mutual and external disturbances, the actual state constraints may not be satisfied. The following theorem shows that the constraint tightening approach designed in (7) can address the problem.

Theorem 1: Suppose that Assumptions 1-5 hold. Then, under Algorithm 1, the actual state satisfies $x_i(k) \in \mathcal{X}_i$ $\forall k > 0, i \in \mathcal{M}$.

Proof: According to Algorithm 1, the actual state trajectory is generated by applying the control input signals between two successive triggering instants. Therefore, proving Theorem 1 is equivalent to proving $x_i(k_i^r + m) \in \mathcal{X}_i$ $\forall m = 1, \ldots, \Delta(k_i^{r+1}), i \in \mathcal{M}$.

This theorem is proved by investigating two cases. *Case 1 ($x(k_i^r) \notin \phi_i(\varepsilon)$ and $x(k_i^r) \in \mathcal{X}_i$):* in this situation, the control input $\hat{\mathbf{u}}_i^*(k_i^r)$ obtained by solving $\mathcal{P}_i$ is applied. From the inequality in (15), we have $\|x_i(k_i^r+m) - \hat{x}_i^*(k_i^r+m|k_i^r)\|_{P_i} \leq \tau_i$ for all $m = 1, \ldots, \Delta(k_i^{r+1})$. Since $\hat{x}_i^*(k_i^r+m|k_i^r) \in \mathcal{X}_i \ominus \mathcal{B}_i(m)$, using the triangle inequality yields $x_i(k_i^r+m) \in \mathcal{X}_i \ominus \mathcal{B}_i(m) \oplus \tau_i \subseteq \mathcal{X}_i$ $\forall m = 1, \ldots, \Delta(k_i^{r+1})$. *Case 2 ($x(k_i^r) \in \phi_i(\varepsilon)$):* in this situation, the control input $\hat{u}_i(k_i^r + m|k_i^r) = K_i(\hat{x}_i(k_i^r + m|k_i^r))$ is applied. We still have $\|x_i(k_i^r + m) - \hat{x}_i(k_i^r + m|k_i^r)\|_{P_i} \leq \tau_i$. According to the equation in (23) and Assumption 4, we can obtain $\hat{x}_i(k_i^r+m|k_i^r) = f_i(\hat{x}_i(k_i^r+m-1|k_i^r), \hat{u}_i(k_i^r+m-1|k_i^r)) +$

$\sum_{j\in\mathcal{N}_i^u} g_{ij}(\tilde{x}_j(k_i^r+m-1|k_i^r)) \in \phi_i(\varepsilon) \subseteq \mathcal{X}_i \ominus \mathcal{B}_i(N_i-1)$. Therefore, utilizing the triangle inequality yields $x_i(k_i^r+m) \in \mathcal{X}_i \ominus \mathcal{B}_i(N_i-1) \oplus \tau_i \subset \mathcal{X}_i$. Combining the above two cases completes this proof. ■

B. Recursive Feasibility Analysis

The recursive feasibility means that $\mathcal{P}_i$ always has a solution for each subsystem $i \in \mathcal{M}$ at every triggering instant provided that an initial feasible solution of $\mathcal{P}_i$ is available. Before giving the technical details, an assumption is given to facilitate the initialization phase.

Assumption 5 [22]: Given the initial states $x(0) = [x_1^T(0), \ldots, x_M^T(0)]^T$, there always exist assumed state trajectory $\tilde{\mathbf{x}}_j(0)$, $j \in \mathcal{N}_i^u$ such that $\mathcal{P}_i$ in (7) has a solution.

Based on Assumption 5, the recursive feasibility is shown in the following theorem.

Theorem 2: For the system (4) with Assumptions 1–5, if the following conditions are satisfied:

$$\sum_{l=0}^{N_i-1} \max\left\{L_{f_i}^l, L_{f_{K_i}}^l\right\}\left(\Gamma_i L_{g_{ij}}\left(N_i\sigma + \tfrac{4\varepsilon}{5\sqrt{M}}\right)\right) + \max\left\{L_{f_i}^{N_i}, L_{f_{K_i}}^{N_i}\right\}\tau_i \le \sigma \tag{24}$$

$$L_{f_i}^{N_i-1}\tau_i + \frac{\left(L_{f_i}^{N_i-1}-1\right)}{L_{f_i}-1} N_i\Gamma_i L_{g_{ij}}\sigma \le \tfrac{\varepsilon}{5\sqrt{M}} \tag{25}$$

$$\sigma \le \tfrac{4(1-c_i)\varepsilon}{5\sqrt{M}} \tag{26}$$

then, the optimization problem $\mathcal{P}_i$ is recursively feasible.

To prove this theorem, the following useful lemmas are given, where Lemma 4 illustrates the satisfaction of the constraint in (7b), Lemma 5 indicates that the tightened constraint in (7c) holds true, and Lemma 6 shows the satisfaction of input constraint in (7d).

Lemma 4: For system (4) with Assumptions 1–5, if $\mathcal{P}_i$ has a feasible solution at k_i^r $\forall i \in \mathcal{M}, r \ge 0$, and the condition in (24) holds, then $\|\bar{x}_i(k_i^{r+1}+m|k_i^{r+1}) - \bar{x}_i^*(k_i^{r+1}+m|k_i^r)\|_{P_i} \le \sigma$ $\forall m = 0, \ldots, N_i$.

Proof: This lemma is proved by investigating two cases.

When $m = 0, \ldots, N_i - \Delta(k_i^{r+1})$, we have $\bar{x}_i^*(k_i^{r+1}+m|k_i^r) = \hat{x}_i^*(k_i^{r+1}+m|k_i^r)$. The two states trajectories $\bar{x}_i(k_i^{r+1}+m|k_i^{r+1})$ and $\hat{x}_i^*(k_i^{r+1}+m|k_i^r)$ are generated by adopting the same control input, thus we iteratively obtain

$$\begin{aligned}
&\left\|\bar{x}_i\left(k_i^{r+1}+1|k_i^{r+1}\right) - \hat{x}_i^*\left(k_i^{r+1}+1|k_i^r\right)\right\|_{P_i} \\
&\le L_{f_i}\left\|\bar{x}_i\left(k_i^{r+1}|k_i^{r+1}\right) - \hat{x}_i^*\left(k_i^{r+1}|k_i^r\right)\right\|_{P_i} + N_i\Gamma_i L_{g_{ij}}\sigma \\
&\le L_{f_i}\tau_i + N_i\Gamma_i L_{g_{ij}}\sigma \\
&\ldots \\
&\left\|\bar{x}_i\left(k_i^{r+1}+m|k_i^{r+1}\right) - \hat{x}_i^*\left(k_i^{r+1}+m|k_i^r\right)\right\|_{P_i} \\
&\le L_{f_i}\left\|\bar{x}_i\left(k_i^{r+1}+m-1|k_i^{r+1}\right) - \hat{x}_i^*\left(k_i^{r+1}+m-1|k_i^r\right)\right\|_{P_i} \\
&\quad + N_i\Gamma_i L_{g_{ij}}\sigma \\
&\le L_{f_i}^m\tau_i + \sum_{l=0}^{m-1} L_{f_i}^l N_i\Gamma_i L_{g_{ij}}\sigma.
\end{aligned} \tag{27}$$

When $m = N_i - \Delta(k_i^{r+1}) + 1, \ldots, N_i$, we have

$$\begin{aligned}
&\left\|\bar{x}_i\left(k_i^r+N_i+1|k_i^{r+1}\right) - \bar{x}_i^*\left(k_i^r+N_i+1|k_i^r\right)\right\|_{P_i} \\
&\le L_{f_{K_i}}\left\|\bar{x}_i\left(k_i^r+N_i|k_i^{r+1}\right) - \hat{x}_i^*\left(k_i^r+N_i|k_i^r\right)\right\|_{P_i} \\
&\quad + \Gamma_i L_{g_{ij}} N_i\sigma + \left\|\sum_{j\in\mathcal{N}_i^u} g_{ij}\left(\tilde{x}_j\left(k_i^{r+1}+N_i|k_i^r\right)\right)\right\|_{P_i}.
\end{aligned}$$

Since $\|\tilde{x}_j(k_i^{r+1}+m|k_i^r)\|_{P_i} \le 4\varepsilon/5\sqrt{M}$, for all $m = N_i - \Delta(k_i^{r+1}) + 1, \ldots, N_i$, we iteratively obtain

$$\begin{aligned}
&\left\|\bar{x}_i\left(k_i^{r+1}+m|k_i^{r+1}\right) - \hat{x}_i^*\left(k_i^{r+1}+m|k_i^r\right)\right\|_{P_i} \\
&\le L_{f_{K_i}}^{m+\Delta_{k_i}-N_i}\left\|\bar{x}_i\left(k_i^r+N_i|k_i^{r+1}\right) - \hat{x}_i^*\left(k_i^r+N_i|k_i^r\right)\right\|_{P_i} \\
&\quad + \sum_{l=0}^{m+\Delta_{k_i}-N_i-1} L_{f_{K_i}}^l\Gamma_i L_{g_{ij}}\left(N_i\sigma + \tfrac{4\varepsilon}{5\sqrt{M}}\right).
\end{aligned}$$

By summarizing the above two cases, it follows:

$$\begin{aligned}
&\left\|\bar{x}_i\left(k_i^{r+1}+m|k_i^{r+1}\right) - \hat{x}_i^*\left(k_i^{r+1}+m|k_i^r\right)\right\|_{P_i} \\
&\le \max\left\{L_{f_i}^m, L_{f_{K_i}}^m\right\}\tau_i \\
&\quad + \sum_{l=0}^{m-1}\max\left\{L_{f_i}^l, L_{f_{K_i}}^l\right\}\Gamma_i L_{g_{ij}}\left(N_i\sigma + \tfrac{4\varepsilon}{5\sqrt{M}}\right)
\end{aligned} \tag{28}$$

where $m = 0, \ldots, N_i$. By virtue of the condition in (24), it follows that $\|\bar{x}_i(k_i^{r+1}+m|k_i^{r+1}) - \hat{x}_i^*(k_i^{r+1}+m|k_i^r)\|_{P_i} \le \sigma$, $m = 0, \ldots, N_i$. ■

Lemma 5: For system (4) with Assumptions 1–5, if $\mathcal{P}_i$ has a feasible solution at k_i^r $\forall i \in \mathcal{M}$ and (25) holds, then the state $\bar{x}_i(k_i^{r+1}+m|k_i^{r+1})$ w.r.t. $\bar{u}_i(k_i^{r+1}+m|k_i^{r+1})$ in (16) or (17) satisfies $\bar{x}_i(k_i^{r+1}+m|k_i^{r+1}) \in \mathcal{X}_i \ominus \mathcal{B}_i(m)$ $\forall m = 1, \ldots, N_i - 1$.

Proof: This claim is proved in two cases.

When $m = 1, \ldots, N_i - \Delta(k_i^{r+1})$, utilizing the result in Lemma 4 and the triangle inequality yields

$$\left\|\bar{x}_i\left(k_i^{r+1}+m|k_i^{r+1}\right)\right\|_{P_i} \le \left\|\hat{x}_i^*\left(k_i^{r+1}+m|k_i^r\right)\right\|_{P_i} + L_{f_i}^m\tau_i + \frac{N_i\Gamma_i\left(L_{f_i}^m-1\right)}{L_{f_i}-1}L_{g_{ij}}\sigma_i. \tag{29}$$

Since $\hat{x}_i^*(k_i^{r+1}+m|k_i^r) \in \mathcal{X}_i \ominus \mathcal{B}_i(m+\Delta(k_i^{r+1}))$, and the definition of $\mathcal{B}_i(m)$ in (9), it follows that:

$$\begin{aligned}
\bar{x}_i\left(k_i^{r+1}+m|k_i^{r+1}\right) &\in \mathcal{X}_i \ominus \mathcal{B}_i\left(m+\Delta\left(k_i^{r+1}\right)\right) \\
&\quad \oplus \left(L_{f_i}^m\tau_i + \frac{N_i\Gamma_i\left(L_{f_i}^m-1\right)}{L_{f_i}-1}L_{g_{ij}}\sigma_i\right) \\
&\subset \mathcal{X}_i \ominus \mathcal{B}_i(m).
\end{aligned} \tag{30}$$

When $m = N_i - \Delta(k_i^{r+1}) + 1, \ldots, N_i - 1$, substituting $m = N_i - \Delta(k_i^{r+1})$ into (27) yields

$$\left\|\bar{x}_i\left(k_i^r+N_i|k_i^{r+1}\right) - \hat{x}_i^*\left(k_i^r+N_i|k_i^r\right)\right\|_{P_i} \le L_{f_i}^{N_i-\Delta\left(k_i^{r+1}\right)}\tau_i + \frac{\left(L_{f_i}^{N_i-\Delta\left(k_i^{r+1}\right)}-1\right)}{L_{f_i}-1}N_i\Gamma_i L_{g_{ij}}\sigma. \tag{31}$$

Since $\|\hat{x}_i^*(k_i^r+N_i|k_i^r)\|_{P_i}\le 4\varepsilon/5\sqrt{M}$, according to the condition in (25), it follows that $\|\bar{x}_i(k_i^r+N_i|k_i^{r+1})\|_{P_i}\le\varepsilon/\sqrt{M}$, that is, $\bar{x}_i(k_i^r+N_i|k_i^{r+1})\in\phi_i(\varepsilon)$, which guarantees that the state feedback gain K_i is allowed to be applied during $[k_i^r+N_i, k_i^{r+1}+N_i-1]$. Then, by virtue of Assumption 4, we have $\bar{x}_i(k_i^{r+1}+m|k_i^{r+1})\in\phi_i(\alpha_i\varepsilon)\subset X_i\ominus\mathcal{B}_i(m)$, for all $m=N_i-\Delta(k_i^{r+1})+1,\ldots,N_i-1$. ■

Lemma 6: Suppose that Assumptions 1–5, and the condition in (25) hold. For any $i\in\mathcal{M}$, if $\mathcal{P}_i$ has a solution at k_i^r, then $\bar{u}_i(k_i^{r+1}+m|k_i^{r+1})\in\mathcal{U}_i\ \forall m=0,\ldots,N_i-1$.

Proof: From (16), we obtain $\bar{u}_i(k_i^{r+1}+m|k_i^{r+1})=\hat{u}_i^*(k_i^{r+1}+m|k_i^r)\in\mathcal{U}_i\ \forall m=0,\ldots,N_i-\Delta(k_i^{r+1})-1$. Then, it needs to show that $\bar{u}_i(k_i^{r+1}+m|k_i^{r+1})\in\mathcal{U}_i\ \forall m=N_i-\Delta(k_i^{r+1}),\ldots,N_i-1$. Invoking Lemma 5, we know that $\bar{x}_i(k_i^{r+1}+m|k_i^{r+1})\in\phi_i(\varepsilon)\ \forall m=N_i-\Delta(k_i^{r+1}),\ldots,N_i-1$. Since $\phi_i(\varepsilon)$ is a constraint admissible set according to Lemma 1, we obtain that $\bar{u}_i(k_i^{r+1}+m|k_i^{r+1})=K_i\bar{x}_i(k_i^{r+1}+m|k_i^{r+1})\in\mathcal{U}_i\ \forall m=N_i-\Delta(k_i^{r+1}),\ldots,N_i-1$. Thus, the control input constraint is satisfied. ■

Based on the above lemmas, Theorem 2 can then be proved.

Proof of Theorem 2: This proof follows by induction principle. At time $k=0$, $\mathcal{P}_i$ is feasible with Assumption 5. Now, suppose that $\mathcal{P}_i$ is feasible at any $k_i^r, r>0, i\in\mathcal{M}$. It remains to show that the constructed control input sequence $\bar{\mathbf{u}}_i(k_i^{r+1})$ and the corresponding state sequence $\bar{\mathbf{x}}_i(k_i^{r+1})$ are also feasible for the optimization problem $\mathcal{P}_i$, which can be proved by showing the fact that $\bar{\mathbf{u}}_i(k_i^{r+1})$ and $\bar{\mathbf{x}}_i(k_i^{r+1})$ satisfy the constraints in (7). From the above lemmas, the constraint in (7b) and (7c) holds that follows from Lemmas 4 and 5, respectively, and the control input constraint satisfaction in (7d) is shown in Lemma 6. Finally, it remains to show the terminal constraint in (7e) is satisfied. By using the triangle inequality, one obtains

$$\begin{aligned}&\left\|\bar{x}_i\left(k_i^{r+1}+N_i|k_i^{r+1}\right)\right\|_{P_i}\\&\le\left\|\bar{x}_i\left(k_i^{r+1}+N_i|k_i^{r+1}\right)-\hat{x}_i^*\left(k_i^{r+1}+N_i|k_i^r\right)\right\|_{P_i}\\&\quad+\left\|\hat{x}_i^*\left(k_i^{r+1}+N_i|k_i^r\right)\right\|_{P_i}.\end{aligned}\tag{32}$$

Since $\hat{x}_i^*(k_i^r+N_i|k_i^r)\in\phi_i(4\varepsilon/5)$, we obtain $\|\hat{x}_i^*(k_i^{r+1}+N_i|k_i^r)\|_{P_i}\le 4c_i\varepsilon/5\sqrt{M}$ from the property 2) in Assumption 4. Then, by application of the condition in (26), the terminal constraint $\bar{x}_i(k_i^{r+1}+N_i|k_i^{r+1})\le 4\varepsilon/5\sqrt{M}$ can be satisfied. Incorporating the above lemmas completes Theorem 2. ■

Remark 6: From the conditions in (24) and (25), it can be seen that a larger Lipschitz constant L_{f_i} gives rise to a smaller feasible N_i and τ_i, leading to a conservative result. Compared with the conditions for ensuring the event-triggered algorithm feasibility in [22] where the Lipschitz constant L_{f_i} of each subsystem is chosen as a common large upper bound, the conditions in (24) and (25) allow the Lipschitz constants to chosen separately for each subsystem by taking the different characteristics of subsystems into consideration. Therefore, the designed conditions enjoy lower conservativeness.

C. Stability Analysis

In this part, closed-loop stability under Algorithm 1 is analyzed by the following theorem.

Theorem 3: Suppose that Assumptions 1–5 hold, and conditions in (24), (25), and (26) are satisfied. Then, the overall system (4) under Algorithm 1 is stable, provided that the following conditions hold:

$$\tau_i+(N_i-1)\sigma<\tfrac{\varepsilon}{5\sqrt{M}}\tag{33}$$

$$\tau_i\le\tfrac{(1-\alpha_i)\varepsilon}{\sqrt{M}}.\tag{34}$$

Proof: The core of proving Theorem 3 is to show two claims. *(C1):* all states $x, x\notin\phi(\varepsilon)$ will enter $\phi(\varepsilon)$ in finite time and *(C2):* the states x never leave $\phi(\varepsilon)$ forever once they enter $\phi(\varepsilon)$. These two claims can be obtained by proving that the state trajectory $x_i(k)$ can enter $\phi_i(\varepsilon)$ in finite time and never leave $\phi_i(\varepsilon)$ [10].

(C1): For this claim, we need to verify two points, that is: (P1) based on the triggering condition (19), the state trajectory $x_i(k)$ can enter $\phi_i(\varepsilon)$ in finite time and (P2) the parallel-triggering condition (21) can still make the state trajectory $x_i(k)$ enter $\phi_i(\varepsilon)$ in finite time.

We show (P1) by following the similar idea in [26] and [27]. Use $\bar{k}_i^r$ to denote the rth triggering instants of subsystem i determined only by the triggering condition (19). Two cases are considered.

Case I: If no event occurs at time k, in Section III-B, we have shown that $V_i(\bar{x}_i(k|k))-V_i(\hat{x}_i^*(\bar{k}_i^r|\bar{k}_i^r))<0$ and $V_i(\bar{x}_i(k|k))-V_i(\bar{x}_i(k-1|k-1))<0$, $\bar{k}_i^r\le k<\bar{k}_i^{r+1}$.

Case II: If an event occurs at time k (without loss of generality, set $k=\bar{k}_i^{r+1}$), the difference of the Lyapunov function candidate, that is, $V_i(\hat{x}_i^*(\bar{k}_i^{r+1}|\bar{k}_i^{r+1}))-V_i(\bar{x}_i(\bar{k}_i^{r+1}-1|\bar{k}_i^{r+1}-1))$ and $V_i(\hat{x}_i^*(\bar{k}_i^{r+1}|\bar{k}_i^{r+1}))-V_i(\hat{x}_i^*(\bar{k}_i^r|\bar{k}_i^r))$, are calculated as

$$\begin{aligned}&V_i\left(\hat{x}_i^*\left(\bar{k}_i^{r+1}|\bar{k}_i^{r+1}\right)\right)-V_i\left(\bar{x}_i\left(\bar{k}_i^{r+1}-1|\bar{k}_i^{r+1}-1\right)\right)\\&\le-\left\|x_i\left(\bar{k}_i^{r+1}-1\right)\right\|_{P_i}+\left\|x_i\left(\bar{k}_i^{r+1}\right)-\bar{x}_i\left(\bar{k}_i^{r+1}|\bar{k}_i^{r+1}-1\right)\right\|_{P_i}\\&\quad+\sum_{m=1}^{N_i-1}\left\|\hat{x}_i^*\left(\bar{k}_i^{r+1}+m|\bar{k}_i^{r+1}\right)-\bar{x}_i\left(\bar{k}_i^{r+1}+m|\bar{k}_i^{r+1}-1\right)\right\|_{P_i}\\&\quad+\left\|\bar{x}_i\left(\bar{k}_i^{r+1}+N_i|\bar{k}_i^{r+1}\right)\right\|_{P_i}.\end{aligned}$$

Since $\|\hat{x}_i^*(\bar{k}_i^{r+1}+m|\bar{k}_i^{r+1})-\bar{x}_i(\bar{k}_i^{r+1}+m|\bar{k}_i^{r+1}-1)\|_{P_i}\le\|\hat{x}_i^*(\bar{k}_i^{r+1}+m|\bar{k}_i^{r+1})-\hat{x}_i^*(\bar{k}_i^r+m|\bar{k}_i^r)\|_{P_i}\le\sigma$, $\bar{x}_i(\bar{k}_i^{r+1}+N_i|\bar{k}_i^{r+1})\in\phi_i(4\varepsilon/5)$ and $x_i(\bar{k}_i^{r+1}-1)\notin\phi_i(\varepsilon)$, we have

$$\begin{aligned}&V_i\left(\hat{x}_i^*\left(\bar{k}_i^{r+1}|\bar{k}_i^{r+1}\right)\right)-V_i\left(\bar{x}_i\left(\bar{k}_i^{r+1}-1|\bar{k}_i^{r+1}-1\right)\right)\\&\le-\tfrac{\varepsilon}{\sqrt{M}}+\tau_i+(N_i-1)\sigma+\tfrac{4\varepsilon}{5\sqrt{M}}.\end{aligned}$$

Therefore, if the condition in (33) holds, one obtains

$$V_i\left(\hat{x}_i^*\left(\bar{k}_i^{r+1}|\bar{k}_i^{r+1}\right)\right)-V_i\left(\bar{x}_i\left(\bar{k}_i^{r+1}-1|\bar{k}_i^{r+1}-1\right)\right)<0.\tag{35}$$

Similarly, we obtain $V_i(\hat{x}_i^*(\bar{k}_i^{r+1}|\bar{k}_i^{r+1}))-V_i(\hat{x}_i^*(\bar{k}_i^r|\bar{k}_i^r))<0$. Thus, $\Delta V_i(k)<0\ \forall k>0$, which implies that the state $x_i(k)$ enters the terminal set $\phi_i(\varepsilon)$ in finite time [26], [27].

We show (P2) by contradiction. Note that the triggering rule is that an event will be triggered only when both (21a) and (21b) are satisfied. Suppose that there does not exist a finite k such that the subsystem state $x_i(k)\in\phi_i(\varepsilon)$, $\phi_i(\varepsilon):=\{x_i:\|x_i\|_{P_i}\le\varepsilon/\sqrt{M}\}$ under the triggering condition in (21). Then $\forall k>0$, there always exists some $\epsilon>0$ such

that $\|x_i(k)\|_{P_i} \geq \varepsilon/\sqrt{M}+\epsilon$. Let k^* represent the time instant when $\varepsilon/\sqrt{M}+\epsilon \geq e^{-\gamma_i k}\|x_i(0)\|_{P_i}+\delta_i$ holds for $k \geq k^*$, then $\|x_i(k)\|_{P_i} > e^{-\gamma_i k}\|x_i(0)\|_{P_i}+\delta_i$ holds for all $k > k^*$, that is, the condition in (21b) holds for all $k > k^*$. Therefore, when $k > k^*$, whether the event is triggered or not depends only on the condition (21a). In other words, when $k > k^*$, the event triggered by the triggering condition in (19) is same as that by the triggering condition in (21). In view of the above supposition, we know that there does not exist a finite time k such that $x_i(k) \in \phi_i(\varepsilon)$, which contradicts (P1).

(C2): Once the state enters the level set $\phi_i(\varepsilon)$, the predicted control input is generated by using the state feedback gain K_i according to (23). Then, the estimated error is bounded by $\|x_i(k_i^r+m)-\hat{x}_i(k_i^r+m|k_i^r)\|_{P_i} \leq \tau_i$. Since $\hat{x}_i(k_i^r+m|k_i^r) \in \phi_i(\alpha_i\varepsilon)$ according to Assumption 4, by virtue of the condition in (34), we have $\|x_i(k_i^p+m)\|_{P_i} \leq \varepsilon/\sqrt{M}$. This implies that the actual state never leaves $\phi(\varepsilon)$ even if the event is triggered in the terminal set.

Summarizing (C1) and (C2) completes the proof. ■

Remark 7: From (C1), we can see that the parallel-triggering condition (21) no longer needs to keep the Lyapunov function decreasing all the time. Suppose that at $\bar{k}_i^r$, the condition in (21a) holds, but the condition in (21b) does not, then the event is not triggered and the Lyapunov function candidate may not keep decreasing. Until $k_i^r, k_i^r > \bar{k}_i^r$, both (21a) and (21b) hold, the event is triggered. Therefore, the Lyapunov function candidate may no longer keep decreasing during $[\bar{k}_i^r, k_i^r)$.

Remark 8: Theorem 3 implies that the closed-loop stability is related to the prediction horizon N_i, and the control parameter σ and τ_i.

1) From (25) and (33), one observes that a larger τ_i forces smaller values of σ and N_i, which in turn impacts the feasibility and the closed-loop stability, although a larger τ_i can bring economical communication load.
2) From (24), (25), and (33), it can be derived that due to the use of Lipschitz constants, a larger prediction horizon N_i leads to smaller σ and τ_i, resulting in a more conservative result, although a larger N_i has the potential to improve the control performance.
3) To choose these control parameters, one can first determine the feasible range for σ and τ_i according to (26) and (34), and then select an appropriate N_i based on (24), (25), and (33).

V. Simulations

This section validates the effectiveness of the proposed event-triggered DMPC algorithm by an example that contains three mass-spring-damper subsystems connected to each other with springs as in [5]. The structure diagram of the system is displayed in Fig. 3.

The discretized version of the dynamic of the three carts, which are obtained by forward-Euler discretized method, is expressed as

$$\begin{aligned}
x_{11}(k+1) &= x_{11}(k)+Tx_{12}(k)\\
x_{12}(k+1) &= \left(1-\tfrac{Th_1}{m_1}\right)x_{12}(k)-\tfrac{Tk_1}{m_1}e^{-x_{11}(k)}x_{11}(k)\\
&\quad -\tfrac{Tk_c}{m_1}(x_{11}(k)-x_{21}(k))+\tfrac{T}{m_1}u_1+w_1(k)\\
x_{21}(k+1) &= x_{21}(k)+Tx_{22}(k)\\
x_{22}(k+1) &= \left(1-\tfrac{Th_2}{m_2}\right)x_{22}(k)-\tfrac{Tk_2}{m_2}e^{-x_{21}(k)}x_{21}(k)\\
&\quad -\tfrac{Tk_c}{m_2}(x_{21}(k)-x_{11}(k))-\tfrac{Tk_c}{m_2}(x_{21}(k)\\
&\quad -x_{31}(k))+\tfrac{T}{m_2}u_2+w_2(k)\\
x_{31}(k+1) &= x_{31}(k)+Tx_{32}(k)\\
x_{32}(k+1) &= \left(1-\tfrac{Th_3}{m_3}\right)x_{32}(k)-\tfrac{Tk_3}{m_3}e^{-x_{31}(k)}x_{31}(k)\\
&\quad -\tfrac{Tk_c}{m_3}(x_{31}(k)-x_{21}(k))+\tfrac{T}{m_3}u_3+w_3(k)
\end{aligned}$$

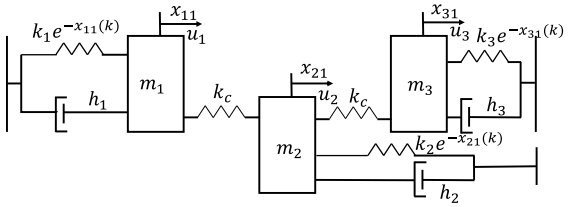

Fig. 3. Structure diagram of the simulated system.

TABLE I
Parameters Description

Parameters	Value	Parameters	Value
m_1	1 kg	m_2	1 kg
m_3	1.25 kg	k_1	0.8 N/m
k_2	0.15 N/m	k_3	0.5 N/m
k_c	0.015 N/m	h_1	1.2 Ns/m
h_2	1.2 Ns/m	h_3	0.42 Ns/m

where the component x_{i1} and the component x_{i2} are the displacement and the velocity of cart $i, i = 1, 2, 3$, respectively. The stiffness of the local nonlinear spring and the local viscous damping of each cart i is k_i and h_i, respectively. The stiffness of the interconnecting springs is k_c. $u_i(k)$ and $w_i(k)$ are the control input and the disturbance for cart i, whose mass is m_i. T is the sampling time, which can be set to $T = 0.2$ s according to [35]. The value of these system parameters is given in Table I. The state and control input constraints of each cart are set as $\mathcal{X}_i = \{x_i : -1 \leq x_{i1} \leq 1, -1 \leq x_{i2} \leq 1\}$ and $\mathcal{U}_i = \{u_i : -1 \leq u_i \leq 1\}$. The initial states are $x_1(0) = (0.6, 0)$, $x_1(0) = (-0.5, 0)$, and $x_1(0) = (0.5, 0)$, respectively.

To implement Algorithm 1, the weighted matrices are set as $Q_i = \begin{bmatrix}0.2 & 0\\ 0 & 0.2\end{bmatrix}$, $R_i = 0.1$, $i = 1, 2, 3$. The feedback gains are calculated as $K_1 = [-0.6290 \quad -0.9871]$, $K_2 = [-1.0655 \quad -1.1210]$, $K_3 = [-0.7823 \quad -1.6816]$ by using the LQR method. To satisfy Assumption 3, ΔQ_i are set as $\Delta Q_i = \begin{bmatrix}0.2 & 0\\ 0 & 0.4\end{bmatrix}$, and the corresponding terminal matrixes are calculated as $P_1 = \begin{bmatrix}3.3776 & 0.9837\\ 0.9837 & 1.5419\end{bmatrix}$, $P_2 = \begin{bmatrix}3.6225 & 1.2289\\ 1.2289 & 1.5905\end{bmatrix}$, and $P_3 = \begin{bmatrix}3.6424 & 1.3692\\ 1.3692 & 2.4882\end{bmatrix}$. Thus, the Lipschitz constants are $L_{f_1} = 1.1402$, $L_{f_2} = 1.0430$, and $L_{f_3} = 1.1556$. According to Lemma 1, the control parameter is designed as $\varepsilon = 0.9486$, and $\alpha_i = 0.9$. Then, according to the conditions in (20), (26), and (34), the other control parameters are designed as $\delta_1 = \delta_2 = \delta_3 = 0.5$, $\sigma = 0.02$, $\tau_1 = 0.0027$, $\tau_2 = 0.0021$, and $\tau_3 = 0.0023$. Finally, the prediction horizon

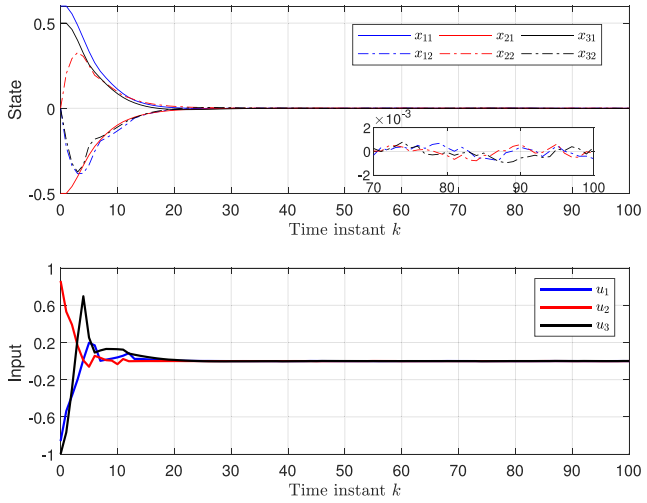

Fig. 4. State and input trajectories of each cart.

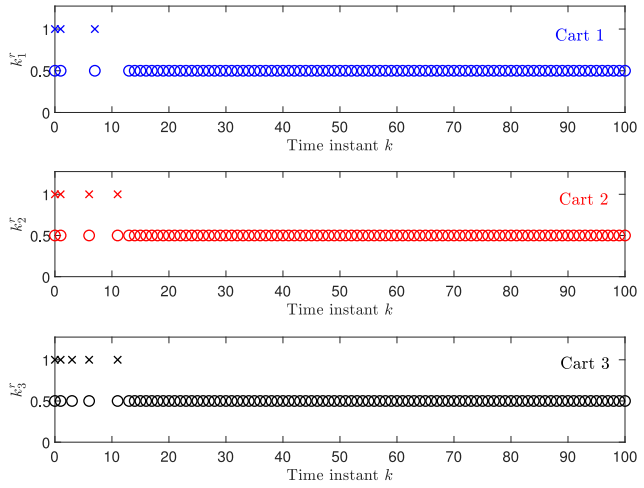

Fig. 5. Triggering instants ("×") and transmission instants ("○") under the algorithm in [22].

are given by $N_2 = 6$, $N_2 = N_3 = 5$ based on the conditions in (24), (25), and (33). The disturbance bounds of the three carts are $\rho_1 = \rho_2 = \rho_3 = 0.001$.

The displacements, velocities, and control inputs of the three carts under Algorithm 1 are shown in Fig. 4, respectively. It can be observed that the actual state constraints and the control inputs constraints are satisfied, and the closed-loop system is stable. To illustrate the advantages of the proposed Algorithm 1 in reducing computation and communication loads, the triggering instants and transmission instants under the proposed Algorithm 1 and the algorithm in [22] are shown in Figs. 5 and 6, respectively. Note that the consumption of the computation resources caused by $u = Kx$ can be ignored, the total number of triggering and transmission instants can represent the consumption of the computation and communication resources, respectively. It can be seen that among all 300 steps, the total number of the triggering and transmission instants are 12 and 276 in Fig. 5, while 11 and 67 in Fig. 6, respectively. We can see that the proposed compound event-triggered DMPC enjoys lower computation and communication loads compared with the algorithm in [22].

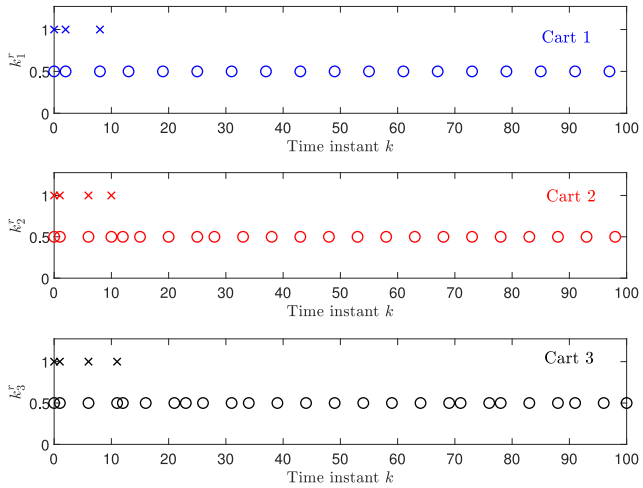

Fig. 6. Triggering instants ("×") and transmission instants ("○") under Algorithm 1.

VI. Conclusion

In this article, event-triggered DMPC for coupled nonlinear systems subject to external disturbances has been studied. A compound event-triggered DMPC strategy has been proposed accordingly, including a compound triggering condition and a new constraint tightening approach. In this strategy, the number of triggering instants associated with the computation and communication load has been reduced significantly, and the actual state constraints have been satisfied. Sufficient conditions to guarantee the recursive feasibility of the proposed algorithm and the stability of the closed-loop system have been derived. The effectiveness of the proposed strategy has been validated by a simulation example.

Appendix
Proof of Lemma 2

The estimated error between the predicted state and the actual one at the next triggering instant k_i^{r+1} is calculated as

$$\begin{aligned}&\left\|x\left(k_i^{r+1}\right)-\hat{x}_i^*\left(k_i^{r+1}|k_i^r\right)\right\|_{P_i}\\&\le L_{f_i}\left\|x_i\left(k_i^{r+1}-1\right)-\hat{x}_i^*\left(k_i^{r+1}-1|k_i^r\right)\right\|_{P_i}+\rho_i\\&\quad+\left\|\sum_{j\in\mathcal{N}_i^u}g_{ij}\left(x_j\left(k_i^{r+1}-1\right)\right)-\sum_{j\in\mathcal{N}_i^u}g_{ij}\left(\tilde{x}_j\left(k_i^{r+1}-1|k_i^r\right)\right)\right\|_{P_i}\end{aligned}\tag{36}$$

where

$$\begin{aligned}&\left\|\sum_{j\in\mathcal{N}_i^u}g_{ij}\left(x_j\left(k_i^{r+1}-1\right)\right)-\sum_{j\in\mathcal{N}_i^u}g_{ij}\left(\tilde{x}_j\left(k_i^{r+1}-1|k_i^r\right)\right)\right\|_{P_i}\\&\le\Gamma_i L_{g_{ij}}\left(\left\|x_j\left(k_i^{r+1}-1\right)-\hat{x}_j^*\left(k_i^{r+1}-1|\eta_j(k_i^{r+1}-1)\right)\right\|_{P_i}\right.\\&\quad\left.+\left\|\hat{x}_j^*\left(k_i^{r+1}-1|\eta_j\left(k_i^{r+1}-1\right)\right)-\tilde{x}_j\left(k_i^{r+1}-1|k_i^r\right)\right\|_{P_i}\right)\\&\le\Gamma_i L_{g_{ij}}\left(\left\|x_j\left(k_i^{r+1}-1\right)-\hat{x}_j^*\left(k_i^{r+1}-1|k_i^r\right)\right\|_{P_i}+N_i\sigma\right).\end{aligned}\tag{37}$$

From the triggering condition in (14), the following inequality can be obtained:

$$\left\|x_i\left(k_i^{r+1}-1\right)-\hat{x}_i^*\left(k_i^{r+1}-1|k_i^r\right)\right\|_{P_i}\leq\frac{\tau_i-\rho_i-\Gamma_i L_{g_{ij}}(\tau_j+N_i\sigma)}{L_{f_i}}. \tag{38}$$

Substituting (37) and (38) into (36) yields

$$\left\|x\left(k_i^{r+1}\right)-\hat{x}_i^*\left(k_i^{r+1}|k_i^r\right)\right\|_{P_i}\leq\tau_i$$

which completes the proof.

Appendix B
Proof of Lemma 3

For $k=k_i^r+1$, $V_i(\hat{x}_i^*(k_i^r|k_i^r))$ has been obtained at time k_i^r based on the optimal state sequence $\hat{\mathbf{x}}^*{}_i(k_i^r)$, then

$$\begin{aligned}
&V_i(\bar{x}_i(k|k))-V_i\left(\hat{x}_i^*\left(k_i^r|k_i^r\right)\right)\\
&=-\left\|\hat{x}_i^*\left(k_i^r|k_i^r\right)\right\|_{P_i}+\|x_i(k)\|_{P_i}-\left\|\hat{x}_i^*\left(k|k_i^r\right)\right\|_{P_i}\\
&\quad+\underbrace{\sum_{m=1}^{N_i-1}\left(\|\bar{x}_i(k+m|k)\|_{P_i}-\left\|\hat{x}_i^*\left(k+m|k_i^r\right)\right\|_{P_i}\right)}_{\Delta_1}\\
&\quad+\underbrace{\|\bar{x}_i(k+N_i|k)\|_{P_i}-\left\|\hat{x}_i\left(k+N_i|k_i^r\right)\right\|_{P_i}}_{\Delta_2}+\left\|\hat{x}_i\left(k+N_i|k_i^r\right)\right\|_{P_i}
\end{aligned} \tag{39}$$

where $\hat{x}_i(k+N_i|k_i^r)=f_i(\hat{x}_i^*(k+N_i-1|k_i^r),K_i\hat{x}_i^*(k+N_i-1|k_i^r))+\sum_{j\in\mathcal{N}_i^u}g_{ij}(\tilde{x}_j(k+N_i-1|k_i^r))$.

For Δ_1, by virtue of Assumption 1 and the constructed control input in (16), we iteratively obtain

$$\begin{aligned}
&\left\|\bar{x}_i(k+m|k)-\hat{x}_i^*\left(k+m|k_i^r\right)\right\|_{P_i}\\
&\leq L_{f_i}\left\|\bar{x}_i(k+m-1|k)-\hat{x}_i^*\left(k+m-1|k_i^r\right)\right\|_{P_i}\\
&\quad+\sum_{j\in\mathcal{N}_i^u}L_{g_{ij}}\left\|\tilde{x}_j(k+m-1|k)-\tilde{x}_j\left(k+m-1|k_i^r\right)\right\|_{P_i}\\
&\cdots\\
&\leq L_{f_i}^m e_i(k)+\sum_{j\in\mathcal{N}_i^u}\sum_{l=0}^{m-1}L_{f_i}^{m-l-1}L_{g_{ij}}\xi_j(k+l|k)\\
&=:\chi_i(m)
\end{aligned} \tag{40}$$

where $e_i(k)=\|x_i(k)-\hat{x}_i^*(k|k_i^r)\|_{P_i}$, and $\xi_j(k+l|k)=\|\tilde{x}_j(k+l|k)-\tilde{x}_j(k+l|k_i^r)\|_{P_i}$.

For Δ_2, we obtain

$$\begin{aligned}
\Delta_2&\leq L_{f_{K_i}}\left\|\bar{x}_i(k+N_i-1|k)-\hat{x}_i^*\left(k+N_i-1|k_i^r\right)\right\|_{P_i}\\
&\quad+\sum_{j\in\mathcal{N}_i^u}L_{g_{ij}}\left\|\tilde{x}_j(k+N_i-1|k)-\tilde{x}_j\left(k+N_i-1|k_i^r\right)\right\|_{P_i}.
\end{aligned}$$

Using (40) yields

$$\Delta_2\leq L_{f_{K_i}}\chi_i(N_i-1)+\sum_{j\in\mathcal{N}_i^u}L_{g_{ij}}\xi_j(k+N_i-1|k). \tag{41}$$

Combining (39) with (40) and (41) yields

$$\begin{aligned}
&V_i(\bar{x}_i(k|k))-V_i\left(\hat{x}_i^*\left(k_i^r|k_i^r\right)\right)\\
&\leq-\left\|\hat{x}_i^*\left(k_i^r|k_i^r\right)\right\|_{P_i}+\sum_{m=1}^{N_i-1}\chi_i(m)+\left\|\hat{x}_i\left(k+N_i|k_i^r\right)\right\|_{P_i}\\
&\quad+e_i(k)+L_{f_{K_i}}\chi_i(N_i-1)+\sum_{j\in\mathcal{N}_i^u}L_{g_{ij}}\xi_j(k+N_i-1|k).
\end{aligned}$$

For $k_i^r+1<k<k_i^{r+1}$, the future control input sequence $\bar{\mathbf{u}}_i(k)$ is applied to the subsystem and $V_i(\bar{x}_i(k-1|k-1))$ is obtained. Similarly, we can also obtain the difference between $V_i(\bar{x}_i(k|k))$ and $V_i(\bar{x}_i(k-1|k-1))$ as

$$\begin{aligned}
&V_i(\bar{x}_i(k|k))-V_i(\bar{x}_i(k-1|k-1))\\
&\leq-\|x_i(k-1)\|_{P_i}+\|x_i(k)-\bar{x}_i(k|k-1)\|_{P_i}\\
&\quad+\sum_{m=1}^{N_i-1}\|\bar{x}_i(k+m|k)-\bar{x}_i(k+m|k-1)\|_{P_i}\\
&\quad+\|\bar{x}_i(k+N_i|k)\|_{P_i}-\left\|\hat{x}_i(k+N_i|k-1)\right\|_{P_i}\\
&\quad+\left\|\hat{x}_i(k+N_i|k-1)\right\|_{P_i}
\end{aligned} \tag{42}$$

where $\hat{x}_i(k+N_i|k-1)=f_i(\bar{x}_i(k+N_i-1|k-1),K_i\bar{x}_i(k+N_i-1|k-1))+\sum_{j\in\mathcal{N}_i^u}g_{ij}(\tilde{x}_j(k+N_i-1|k-1))$.

Following a similar technique as the above, we obtain:

$$\begin{aligned}
&V_i(\bar{x}_i(k|k))-V_i(\bar{x}_i(k-1|k-1))\\
&\leq-\|x_i(k-1)\|_{P_i}+\sum_{m=1}^{N_i-1}\chi_i(m)+\left\|\hat{x}_i(k+N_i|k-1)\right\|_{P_i}\\
&\quad+e_i(k)+L_{f_{K_i}}\chi_i(N_i-1)+\sum_{j\in\mathcal{N}_i^u}L_{g_{ij}}\xi_j(k+N_i-1|k)
\end{aligned}$$

where $e_i(k)=\|x_i(k)-\bar{x}_i(k|k-1)\|_{P_i}$, $\xi_j(k+l|k)=\|\tilde{x}_j(k+l|k)-\tilde{x}_j(k+l|k-1)\|_{P_i}$.

References

[1] G. Darivianakis, A. Eichler, and J. Lygeros, "Distributed model predictive control for linear systems with adaptive terminal sets," *IEEE Trans. Autom. Control*, vol. 65, no. 3, pp. 1044–1056, Mar. 2020.

[2] F. Berkel and S. Liu, "An event-triggered cooperation approach for robust distributed model predictive control," *IFAC J. Syst. Control*, vol. 6, pp. 16–24, Dec. 2018.

[3] L. Magni and R. Scattolini, "Stabilizing decentralized model predictive control of nonlinear systems," *Automatica*, vol. 42, no. 7, pp. 1231–1236, 2006.

[4] S. Riverso, M. Farina, and G. Ferrari-Trecate, "Plug-and-play decentralized model predictive control for linear systems," *IEEE Trans. Autom. Control*, vol. 58, no. 10, pp. 2608–2614, Oct. 2013.

[5] X. Liu, Y. Shi, and D. Constantinescu, "Distributed model predictive control of constrained weakly coupled nonlinear systems," *Syst. Control Lett.*, vol. 74, pp. 41–49, Dec. 2014.

[6] P. Segovia, L. Rajaoarisoa, F. Nejjari, E. Duviella, and V. Puig, "A communication-based distributed model predictive control approach for large-scale systems," in *Proc. IEEE 58th Conf. Decis. Control (CDC)*, 2019, pp. 8366–8371.

[7] A. Mirzaei and A. Ramezani, "Cooperative optimization-based distributed model predictive control for constrained nonlinear large-scale systems with stability and feasibility guarantees," *ISA transactions*, vol. 116, pp. 81–96, Oct. 2021.

[8] M. Farina and R. Scattolini, "Distributed predictive control: A non-cooperative algorithm with neighbor-to-neighbor communication for linear systems," *Automatica*, vol. 48, no. 6, pp. 1088–1096, 2012.

[9] A. Ma, K. Liu, Q. Zhang, and Y. Xia, "Distributed MPC for linear discrete-time systems with disturbances and coupled states," *Syst. Control Lett.*, vol. 135, Jan. 2020, Art. no. 104578.

[10] W. B. Dunbar, "Distributed receding horizon control of dynamically coupled nonlinear systems," *IEEE Trans. Autom. Control*, vol. 52, no. 7, pp. 1249–1263, Jul. 2007.
[11] H. Hu, K. Gatsis, M. Morari, and G. J. Pappas, "Non-cooperative distributed MPC with iterative learning," *IFAC-PapersOnLine*, vol. 53, no. 2, pp. 5225–5232, 2020.
[12] L. Dai, Z. Qiang, Z. Sun, T. Zhou, and Y. Xia, "Distributed economic MPC for dynamically coupled linear systems with uncertainties," *IEEE Trans. Cybern.*, early access, Nov. 10, 2020, doi: 10.1109/TCYB.2020.3030021.
[13] P. D. Christofides, R. Scattolini, D. M. De la Pena, and J. Liu, "Distributed model predictive control: A tutorial review and future research directions," *Comput. Chem. Eng.*, vol. 51, pp. 21–41, Apr. 2013.
[14] T. Li, D. Yang, X. Xie, and H. Zhang, "Event-triggered control of nonlinear discrete-time system with unknown dynamics based on HDP (λ)," *IEEE Trans. Cybern.*, early access, Feb. 2, 2021, doi: 10.1109/TCYB.2020.3044595.
[15] R. Koike, T. Endo, and F. Matsuno, "Output-based dynamic event-triggered consensus control for linear multiagent systems," *Automatica*, vol. 133, Nov. 2021, Art. no. 109863.
[16] M. C. F. Donkers and W. P. M. H. Heemels, "Output-based event-triggered control with guaranteed $\mathcal{L}_\infty$-gain and improved and decentralized event-triggering," *IEEE Trans. Autom. Control*, vol. 57, no. 6, pp. 1362–1376, Jun. 2012.
[17] X. Li, Z. Sun, Y. Tang, and H. R. Karimi, "Adaptive event-triggered consensus of multiagent systems on directed graphs," *IEEE Trans. Autom. Control*, vol. 66, no. 4, pp. 1670–1685, Apr. 2021.
[18] H. Li, W. Yan, Y. Shi, and Y. Wang, "Periodic event-triggering in distributed receding horizon control of nonlinear systems," *Syst. Control Lett.*, vol. 86, pp. 16–23, Dec. 2015.
[19] J. Zhan, Y. Hu, and X. Li, "Adaptive event-triggered distributed model predictive control for multi-agent systems," *Syst. Control Lett.*, vol. 134, Dec. 2019, Art. no. 104531.
[20] Y. Zou, X. Su, S. Li, Y. Niu, and D. Li, "Event-triggered distributed predictive control for asynchronous coordination of multi-agent systems," *Automatica*, vol. 99, pp. 92–98, Jan. 2019.
[21] X. Mi, Y. Zou, and S. Li, "Event-triggered MPC design for distributed systems toward global performance," *Int. J. Robust Nonlinear Control*, vol. 28, no. 4, pp. 1474–1495, 2018.
[22] C. Liu, H. Li, Y. Shi, and D. Xu, "Distributed event-triggered model predictive control of coupled nonlinear systems," *SIAM J. Control Optim.*, vol. 58, no. 2, pp. 714–734, 2020.
[23] D. Zhang, S. K. Nguang, and L. Yu, "Distributed control of large-scale networked control systems with communication constraints and topology switching," *IEEE Trans. Syst., Man, Cybern., Syst.*, vol. 47, no. 7, pp. 1746–1757, Jul. 2017.
[24] L. Zhang, J. Wang, Y. Ge, and B. Wang, "Robust distributed model predictive control for uncertain networked control systems," *IET Control Theory Appl.*, vol. 8, no. 17, pp. 1843–1851, 2014.
[25] H. Yang, Y. Li, L. Dai, and Y. Xia, "MPC-based defense strategy for distributed networked control systems under DoS attacks," *Syst. Control Lett.*, vol. 128, pp. 9–18, Jul. 2019.
[26] A. Ma, K. Liu, Q. Zhang, T. Liu, and Y. Xia, "Event-triggered distributed MPC with variable prediction horizon," *IEEE Trans. Autom. Control*, vol. 66, no. 10, pp. 4873–4880, Oct. 2021.
[27] C. Liu, J. Gao, H. Li, and D. Xu, "Aperiodic robust model predictive control for constrained continuous-time nonlinear systems: An event-triggered approach," *IEEE Trans. Cybern.*, vol. 48, no. 5, pp. 1397–1405, May 2018.
[28] M. Wang, J. Sun, and J. Chen, "Input-to-state stability of perturbed nonlinear systems with event-triggered receding horizon control scheme," *IEEE Trans. Ind. Electron.*, vol. 66, no. 8, pp. 6393–6403, Aug. 2019.
[29] D. L. Marruedo, T. Alamo, and E. Camacho, "Input-to-state stable MPC for constrained discrete-time nonlinear systems with bounded additive uncertainties," in *Proc. 41st IEEE Conf. Decis. Control*, vol. 4, 2002, pp. 4619–4624.
[30] P. Li, Y. Kang, Y.-B. Zhao, and T. Wang, "A novel self-triggered MPC scheme for constrained input-affine nonlinear systems," *IEEE Trans. Circuits Syst. II, Exp. Briefs*, vol. 68, no. 1, pp. 306–310, Jan. 2021.
[31] C. Rajhans, S. C. Patwardhan, and H. Pillai, "Discrete time formulation of quasi infinite horizon nonlinear model predictive control scheme with guaranteed stability," *IFAC-PapersOnLine*, vol. 50, no. 1, pp. 7181–7186, 2017.
[32] K. Hashimoto, S. Adachi, and D. V. Dimarogonas, "Distributed aperiodic model predictive control for multi-agent systems," *IET Control Theory Appl.*, vol. 9, no. 1, pp. 10–20, 2014.
[33] X.-M. Sun, X.-F. Wang, Y. Hong, and W. Xia, "Stabilization control design with parallel-triggering mechanism," *IEEE Trans. Ind. Electron.*, vol. 64, no. 4, pp. 3260–3267, Apr. 2017.
[34] J. Yoo and K. H. Johansson, "Event-triggered model predictive control with a statistical learning," *IEEE Trans. Syst., Man, Cybern., Syst.*, vol. 51, no. 4, pp. 2571–2581, Apr. 2021.
[35] T. Wang, Y. Kang, P. Li, Y.-B. Zhao, and P. Yu, "Robust model predictive control for constrained networked nonlinear systems: An approximation-based approach," *Neurocomputing*, vol. 418, pp. 56–65, Dec. 2020.

Yu Kang (Senior Member, IEEE) received the Ph.D. degree in control theory and control engineering from the University of Science and Technology of China, Hefei, China, in 2005.

From 2005 to 2007, he was a Postdoctoral Fellow with the Academy of Mathematics and Systems Science, Chinese Academy of Sciences. He is currently a Professor with the Department of Automation and the Institute of Advanced Technology, University of Science and Technology of China, and the Key Laboratory of Technology in GeoSpatial Information Processing and Application System, Chinese Academy of Sciences, Beijing, China. His current research interests include monitoring of vehicle emissions, adaptive/robust control, variable structure control, mobile manipulator, and Markovian jump systems.

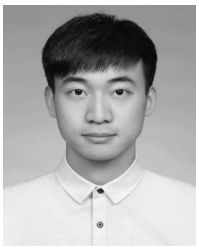

Tao Wang received the B.S. degree from Harbin Engineering University, Harbin, China, in 2018. He is currently pursuing the M.S. degree with the Department of Automation, University of Science and Technology of China, Hefei, China.

His research interests include model predictive control and networked control systems.

Pengfei Li received the Ph.D. degree in control science and engineering from the University of Science and Technology of China (USTC), Hefei, China, in 2020.

He is currently a Postdoctoral Fellow with the School of Information Science and Technology, USTC. His research interests include networked control systems, model predictive control, and learning-based control.

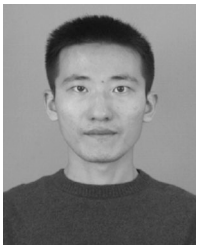

Zhenyi Xu was born in 1993. He received the Ph.D. degree in control science and engineering from the Department of Automation, University of Science and Technology of China, Hefei, China, in 2020.

He is currently a Postdoctoral Fellow with the Institute of Artificial Intelligence, Hefei Comprehensive National Science Center (Anhui Artificial Intelligence Laboratory), Hefei. His research interests are deep learning, urban computing, intelligent transportation, and spatiotemporal data mining.

Yun-Bo Zhao (Senior Member, IEEE) received the B.Sc. degree from Shandong University, Jinan, China, in 2003, the M.Sc. degree from the Key Laboratory of Systems and Control, Chinese Academy of Sciences, Beijing, China, in 2007, and the Ph.D. degree from the University of Glamorgan, Pontypridd, U.K., in 2008.

He is currently a Professor with the Department of Automation, University of Science and Technology of China, Hefei, China. He had worked with INRIA, Paris, France; University of Glasgow, Glasgow, U.K.; and Imperial College London, London, U.K., on various research projects. His main research interests include networked control systems, AI-enabled control, human–machine integrated intelligence, and systems biology.